THE ASTROPHYSICAL JOURNAL SUPPLEMENT SERIES, 65:385–404, 1987 November

A FLUX-LIMITED SAMPLE OF GALACTIC CARBON STARS

M. J. CLAUSSEN AND S. G. KLEINMANN
Department of Physics and Astronomy, University of Massachusetts
R. R. JOYCE
Kitt Peak National Observatory, National Optical Astronomy Observatories[1]
AND
M. JURA
Department of Astronomy, University of California, Los Angeles
Received 1987 March 5; accepted 1987 April 29

ABSTRACT

We summarize the infrared properties of a flux-limited sample of Galactic carbon stars taken from the *Two Micron Sky Survey* (TMSS) to provide estimates of their space distribution and mass-loss rates.

Although 88% of the stars in the sample are optical variables, only a few have 2.2 μm amplitudes exceeding 0.5 mag. Given their relative stability, and the assumption that the Galactic carbon stars have the same observed narrow range of absolute 2.2 μm magnitudes as carbon stars in the Magellanic Clouds, we have determined that the TMSS sample penetrates a volume of radius of 1.5 kpc. The infrared colors of carbon stars are used to test earlier assumptions, that these stars have a narrow range in luminosity at other wavelengths.

The local space density of carbon stars is found to be $\log \rho_0$ (kpc^{-3}) $= 2.0 \pm 0.4$; they appear to be concentrated toward the plane of the Galaxy with an exponential scale height $\log z_0$ (pc) $= 2.3 \pm 0.1$. Thus their surface density is $\log N$ (kpc^{-2}) $= 1.6 \pm 0.2$.

The distribution of mass-loss rates, determined from the derived luminosities and distances, and the observed *IRAS* 60 μm flux densities, shows a peak at 2×10^{-7} $M_\odot$ yr^{-1}. Extrapolating to the entire Galaxy, we derive the total mass-return rate from carbon stars like those found in the TMSS to be 0.013 $M_\odot$ yr^{-1}; the largest contribution comes from stars with the highest infrared amplitudes of variation. If the apparent relationship between infrared amplitude and mass-loss rate exists for heavily dust-enshrouded carbon stars detected only in longer wavelength surveys, then these stars probably contribute far more to the total rate of mass return to the Galaxy than the carbon stars sampled at 2 μm.

From our estimates of the scale heights and the average mass-loss rates of carbon stars seen in the TMSS, we find that the time scale for the carbon star evolutionary phase is between 10^5 and 10^6 yr, and that the main-sequence progenitors to these stars have masses between 1.2 and 1.6 $M_\odot$, which implies that they are descended from F-type stars. At least 10% of all main-sequence F stars eventually pass through the carbon star phase.

Subject headings: galaxies: The Galaxy — infrared: sources — interstellar: matter — stars: carbon — stars: evolution — stars: mass loss — stars: stellar statistics

I. INTRODUCTION

Because of their high luminosities and distinctively red colors, carbon stars can be seen to large distances in this Galaxy and are detected in several members of the Local Group. Surveys of carbon stars in these systems trace the distribution of intermediate-age stars, and provide a means of assessing the contribution of carbon stars to the interstellar medium.

Examination of the large-scale Case objective-prism survey of carbon stars (Stephenson 1973) shows that these stars are strongly concentrated toward the Galactic plane. Details of the distribution of carbon stars within the Galactic plane, as deduced from photographic surveys carried out in the near-infrared, have shown that (1) carbon stars are strongly concentrated in the direction of the Carina spiral arm (Blanco 1965; Westerlund 1971); (2) there is a deficiency in the density of carbon stars in the direction of the Galactic center, especially when compared with M-type stars (Nassau and Blanco 1958; Blanco 1965); and (3) the density of carbon stars in the anticenter direction is greatly enhanced over that found in the direction of the Galactic center, indicating an increase in density of a factor of 3 over galactocentric radii between 5 and 15 kpc (Fuenmayor 1981).

Recently, Thronson *et al.* (1987) analyzed the properties of a group of 619 mid-infrared sources thought to be carbon stars on the basis of their infrared colors (as measured in the *IRAS* survey; *IRAS Point Source Catalog* 1985, hereafter PSC) and refined by removing stars known *not* to be carbon

[1]Operated by the Association of Universities for Research in Astronomy, Inc., under contract to the National Science Foundation.

stars. On the assumption that these stars all have the same intrinsic brightness at 12 μm ($M_{12\ \mu m} = -12.3$ mag, or $L_{12\ \mu m} = 1100\ L_\odot$), and using the fact that most of the stars they studied were brighter than +1.5 mag at 12 μm, Thronson *et al.* (1987) concluded that their sample penetrated to a distance of 6 kpc. In contrast to the optical surveys for carbon stars, these authors found no significant concentration of carbon stars in spiral arms, and no significant gradient with galactocentric distance.

Knowledge of the space distribution and mass-loss rates of carbon stars is required to assess their role in enriching the interstellar medium. The mass of gas in the circumstellar envelopes of carbon stars has been estimated from measurements of their millimeter-wave CO rotational line emission. Knapp *et al.* (1982) and Knapp and Morris (1985) thus analyzed 25 carbon stars having detectable CO emission, and found mass-loss rates ranging from 10^{-7} to $\sim 8\times10^{-5}$ $M_\odot$ yr^{-1}. Olofsson, Eriksson, and Gustafsson (1987) have observed 21 bright N stars, using the millimeter-wave CO emission, finding that 16 have mass-loss rates of a few$\times10^{-7}$ $M_\odot$ yr^{-1}. The mass of dust in the envelopes of carbon stars has been estimated from the brightness of their far-infrared emission. Using an assumed dust emissivity, Jura (1986), Knapp (1985), and Sopka *et al.* (1985) have thus estimated the dust mass-loss rates for the same carbon stars. By comparing these values with the gas masses derived in previous studies, these authors found that the gas-to-dust ratios in the envelopes of carbon stars were relatively constant. Thus the mass-loss rates for the large number of carbon stars detected in *IRAS* and other surveys can be estimated from their dust masses. Initial estimates of the mass-loss rates and space densities of carbon stars suggest that the matter ejected by these stars constitutes a significant fraction of the gas returned to the interstellar medium (Zuckerman *et al.* 1978; Knapp and Morris 1985; Thronson *et al.* 1987).

In this paper, we provide new measures of the space distribution and mass-loss rates of carbon stars, using a flux-limited sample drawn from the *Two Micron Sky Survey* (Neugebauer and Leighton 1969, hereafter TMSS). The sample is expected to be complete, since the TMSS is statistically complete for sources brighter than $m(K) = +3.0$ over the region $-33° < \delta < +81°$, and spectral classifications are now available for almost all of the 5612 sources detected in the TMSS. Baumert (1974) previously identified the majority of the carbon stars in the TMSS by comparing it with the Case survey. This list has been augmented by additional spectroscopic surveys of sources found in the TMSS.

A survey for carbon stars at a wavelength near 2 μm has at least three unique advantages. First, the extinction due to interstellar dust is nearly an order of magnitude less at 2.2 μm than at optical wavelengths; the importance of this effect is underscored by the fact that carbon stars are concentrated within the Milky Way. Second, since the peak in the spectral energy distributions of most carbon stars occurs near 2 μm, their apparent brightness should be relatively insensitive to temperature variations; this effect may help account for the fact that carbon stars observed in the Magellanic Clouds exhibit a small dispersion in *K*-magnitude (see below). Third, the observed emission at 2.2 μm should be relatively unaffected by variations in the masses of the circumstellar envelopes of carbon stars (unless they are large enough to cause appreciable extinction at 2.2 μm), since most of the emission from these cool envelopes occurs at longer wavelengths; thus, compared with a mid-infrared survey, a 2 μm sky survey is less likely to undersample carbon stars having low mass-loss rates.

Much of our analysis rests on the observation that carbon stars found in near-infrared photographic surveys of the Magellanic Clouds show a small dispersion in *K*-magnitude about a mean of $M(K) \sim -8.1$, (e.g., Frogel, Persson, and Cohen 1980). Schechter *et al.* (1987) have also found a small dispersion in absolute *K*-magnitudes of Galactic carbon stars, from an analysis of the rotation curve of the outer Galaxy and their observed radial velocities. If carbon stars in the TMSS have the same narrow range in absolute *K*-magnitude as those seen in the Magellanic Clouds, we deduce that they also have a narrow range in bolometric luminosity, near their average of about 10^4 $L_\odot$ (see below). This luminosity is produced by a core mass of 0.6 $M_\odot$ (Iben and Renzini 1983). At the conclusion of their evolution, the degenerate cores of carbon stars appear as white dwarfs, and the inferred mass for most white dwarfs is near 0.6 $M_\odot$ (Koester, Schulz, and Weidemann 1980). The similarity of these two masses may be the result of mass loss during their asymptotic giant branch evolution (see Mazzitelli and D'Antona 1986).

II. THE SAMPLE

A list of 215 carbon stars in the TMSS is given in Table 1. This extends the 192 stars in the TMSS listed by Baumert (1974). The references listed in column (2) of the table give their spectral classifications. The carbon star classifications of some stars in Table 1 are controversial. For example, Wing and Yorka (1977) have classified TMSS −10104 as an S star, and TMSS 00103, 00123, 00404, and +10154 as SC stars. Bidelman (1980) classifies TMSS −10433 as K5 Ib; TMSS −30106, −30114, 00402, 00418, +10119, +20435, +30074, +50389, +60375, +60409, and +60411 as M-type stars; and +60393 as a blend of M4+C. Similarly, some carbon stars detected in the TMSS may be missing from Table 1, owing to an incorrect classification or identification. For example, Zuckerman and Dyck (1986*b*) have argued that the colors and microwave emission-line strengths of TMSS +60144, which is *not* in Table 1, are consistent with a carbon star classification, but the only spectroscopic observation presently available lists it as an M6 star (Lee *et al.* 1947).

Of the 139 stars in this sample having unambiguous Draper subclasses, 22 are of type R and 117 are of type N. Any distinction between R and N subclasses within this sample may be somewhat artificial, however, since an alternative scheme for classifying carbon stars (Keenan and Morgan 1941) suggests that late-type R and early-type N subclasses overlap (Jaschek 1985).

Associations with named variable stars, infrared sources detected in the RAFGL survey (Price and Murdock 1983), and carbon stars detected in the Case survey (Stephenson 1973) are included in Table 1 in columns (3), (4), and (5), respectively. The next columns give the most accurate available position for each of the sources. In most cases, these

TABLE 1

CARBON STARS IN THE *Two Micron Sky Survey*

TMSS	Spectrum Reference	GCVS/NSV	Case	RAFGL	α (1950)	δ (1950)	Position Reference	TMSS	Spectrum Reference	GCVS/NSV	Case	RAFGL	α (1950)	δ (1950)	Position Reference
+40003	2,3,5,7	SU And	3219		0 2 1.7	+43 16 24	2	+30110	2,3,4,5,7	UV Aur	318	735	5 18 33.31	+32 27 51.4	1
+70003	3,5,7,13	OR Cep	1	12	0 3 36.4	+69 47 22	2	+30114	2,4,5,7	S Aur	336	748	5 23 49.0	+34 6 29	2
+40006	3,5,7	VX And	11	50	0 17 15.1	+44 25 56	2	+10089	2,3,5,7	RT Ori	364		5 30 31.6	+7 7 10	2
+40010	2,3,5,7	AQ And	16	68	0 24 52.5	+35 18 40	2	-30046	2,7	SZ Lep	373	4429S	5 33 45.97	-25 46 09.1	1
+70009	3,5,7	CP Cas	21	86S	0 32 39.1	+70 14 38	2	+20115	4				5 35 12.1	+22 47 31	2
+60026	4,5,7	W Cas	38	4062S	0 51 55.1	+58 17 35	2	+70064	2,3,5,7	S Cam	370		5 35 37.48	+68 46 18.9	1
+60034	3,4,5,7	HO Cas	52	146S	0 59 36.5	+61 35 38	2	-10095	10	NSV 02533		796	5 37 18.4	-8 10 41	2
+50030	3,5,7,14	HV Cas	56	167	1 8 2.4	+53 27 43	2	+10094	3,7	NSV 02557	381	801	5 38 23.4	+12 16 27	2
+60041	4,7	NSV 00438	59	177	1 10 30.3	+62 41 43	2	+20120	2,3,4,5,7	TU Tau	390	812	5 42 9.72	+24 24 1.3	1
+30025	2,3,5,7	Z Psc	63	188	1 13 21.02	+25 30 20.1	1	+20121	2,3,4,5,6,7	Y Tau	393	5168	5 42 40.49	+20 40 33.2	1
-30015	2,5,7	R Scl	68	215	1 24 40.02	-32 48 06.8	1	+40140	11,14,16	NSV 02629		815	5 44 2.7	+43 11 49	2
+60056	3,4,5,7	WW Cas	70	6161S	1 30 17.5	+57 29 44	2	+30127	2,3,4,5,7	FU Aur	402		5 44 55.01	+30 36 53.4	1
+60069	3,4,5,7	X Cas	87	270S	1 53 10.6	+59 0 55	2	+40141	3,5,7	AF Aur	400		5 45 4.1	+44 53 39	2
+50061	3,5,7	BS Per	99		2 23 28.4	+51 53 35	2	-10104	10			4458S	5 56 46.4	-10 52 47	2
-30021	5,7,10	R For	103	337	2 27 01.2	-26 19 13	2	+40151	3,5,7	AZ Aur	433	853	5 57 38.0	+39 40 12	2
+60113	2,3,4,5,7	NSV 01063	131	453	3 7 33.50	+57 42 53.0	1	+30143	2,3,4,5,7	TU Gem	461		6 7 46.81	+26 1 34.7	1
+50088	2,3,5,7	V410 Per	134		3 10 10.2	+47 38 23	2	+10113	3,4,5,7	GK Ori	480	910	6 14 58.2	+8 32 22	2
+50096	3,7,8,11,12,14	V384 Per	142	489	3 22 59.1	+47 21 22	2	+10118	3,4,5,7	BN Mon	498	920	6 19 15.6	+7 22 28	2
+60124	2,3,5,7	U Cam	154	505	3 37 29.09	+62 29 18.8	1	00103	5,10	FU Mon		923	6 19 46.1	+3 27 1	2
+50100	3,4,5,7	NSV 01223	155	507	3 37 47.2	+51 20 37	2	+30150	2,3,5,7	ZZ Gem	501		6 20 56.4	+25 3 31	2
+40067	3,5,7	AC Per	157		3 41 34.9	+44 37 28	2	+10119	7		503		6 21 8.0	+8 30 51	2
+40070	11,14	V414 Per		527	3 48 53.7	+39 43 54	2	-30060	7,10	NSV 02945	507		6 21 39.4	-27 2 19	2
+60138	2,3,5,7	UV Cam	177	4316S	4 1 31.48	+61 39 32.7	1	+10121	2,3,4,5,6,7	BL Ori	508	934	6 22 36.93	+14 45 4.2	1
+30074	3,7		187		4 8 40.9	+29 15 45	2	-10122	14	V636 Mon	933		6 22 38.3	-9 5 32	2
+50115	4,5,7	SY Per	194	558	4 12 46.6	+50 30 9	2	+20145	3,4,5,7	AB Gem	510	937	6 23 17.4	+19 6 14	2
+40089	3,4,5,7	GI Per	215	582	4 26 18.2	+39 45 30	2	+40157	2,3,5,7	RV Aur	529		6 31 10.2	+42 32 37	2
+70055	2,3,5,7	ST Cam	240	633	4 46 01.26	+68 05 01.6	1	+20152	3,4,5,7	CR Gem	534	959	6 31 31.1	+16 6 55	2
+20094	5,7,16	NSV 01737	253		4 47 46.0	+15 42 44	2	+40158	2,3,5,6,7	UU Aur	537	966	6 33 6.64	+38 29 16.1	1
+30098	2,3,5,7	TT Tau	254	639	4 48 22.9	+28 26 35	2	-10133	7,10		542		6 34 43.9	-12 3 9	2
+40101	4,5,7	NSV 01745	257	643	4 49 10.48	+38 25 22.5	1	+30163	2,3,5,7	VW Gem	558		6 38 54.56	+31 30 13.5	1
+50130	3,4,5,7	AU Aur	262	4385S	4 50 25.5	+49 49 09	2	00123	3,10	V372 Mon			6 38 57.7	-4 32 52	2
+20095	3,7		264		4 50 30.3	+22 41 33	2	-20101	10	GM CMa		4521S	6 39 08.2	-22 13 48	2
-10080	2,5,6,7	R Lep	276	667	4 57 19.73	-14 52 47.5	1	00125	4,5,7,10	CZ Mon	573		6 42 3.1	+3 22 7	2
+50135	2,3,5	EL Aur	277	672	4 59 30.60	+50 33 44.6	1	00127	2,3,4,5,7,10	DF Mon	584	4531S	6 45 1.4	+0 44 17	2
00066	2,3,5,6,7	W Ori	284	683	5 2 48.66	+1 6 37.2	1	00131	7,10	NSV 03223	589	1017	6 47 7.8	+3 1 44	2
+40115	2,3,4,5,7	TX Aur	288		5 5 39.1	+38 56 20	2	00136	2,3,4,5,7	GY Mon	609		6 50 42.75	-4 30 48.6	1
-10083	2,5,7	SY Eri	297		5 7 20.88	-5 34 37.6	1	+10144	3,5,7	CL Mon	615	1038	6 52 55.6	+6 26 40	2
+10081	3,5,7	V431 Ori	307	714	5 13 10.0	+11 55 22	2	+10146	2,3,5,7	RV Mon	632	1045	6 55 40.72	+6 14 8.3	1
+40120	2,3,4,5,7	EF Aur	313	4401S	5 15 49.3	+35 44 27	2	00141	2,3,7	V614 Mon	645	1053	6 58 31.88	-3 10 49.7	1
+10083	3,7	NSV 01941	319		5 18 31.0	+7 18 26	2	-10149	4,5,7,10	RY Mon	670	1070	7 4 31.2	-7 28 41	2

TABLE 1—*Continued*

TMSS	Spectrum Reference	GCVS/NSV	Case	RAFGL	α (1950)	δ (1950)	Position Reference
-10152	2,4,5,7	W CMa	676	1075	7 5 43.20	-11 50 35.2	1
+10154	5,7	R CMi	675	4567S	7 5 57.56	+10 6 16.1	1
+10156	2,3,5,7	VX Gem	688	4574S	7 9 58.8	+14 41 18	2
+10158	3,7		695	1092	7 12 59.4	+5 8 59	2
+30182	2,3,5,7	BM Gem	716		7 17 55.9	+25 5 39	2
-20131	7,10,11	NSV 03610	776	1131	7 27 0.6	-19 21 32	2
00158	2,3,5,7,10	BE CMi	815		7 33 53.1	+2 11 31	2
-30097	7,10		846	4621S	7 37 31.9	-27 35 18	2
-10177	5,7,10	GO Pup	897		7 45 16.3	-11 49 42	2
00162	7,10,11,16	V633 Mon	918	1199	7 48 42.4	-2 29 29	2
-30106	7		956		7 53 47.7	-29 20 15	2
-30114	7		1019	1223	8 1 43.8	-31 18 18	2
-20156	2,5,7	RU Pup	1046	4666S	8 5 20.06	-22 46 00.2	1
00172	2,3,5,7,10	RY Hya	1123	1243	8 17 29.8	+2 55 27	2
-20165	5,7,10	AC Pup	1147		8 20 25.9	-15 45 18	2
-30132	7,10		1277		8 41 40.3	-25 25 47	2
-30133	5,7	R Pyx	1285		8 43 23.80	-28 1 4.1	1
-30134	2,7	UZ Pyx	1290		8 44 31.05	-29 32 38.8	1
+20206	2,3,5,6,7	X Cnc	1338	1298	8 52 34.04	+17 25 22.1	1
+20207	3,5,7	T Cnc	1344	1301	8 53 48.91	+20 2 29.8	1
-20184	5,7,10	IQ Hya	1404		9 11 17.3	-23 11 5	2
+10216	5,14	CW Leo		1381	9 45 14.84	+13 30 40.5	3
-20199	2,5,7	Y Hya	1566		9 48 45.00	-22 46 56.9	1
+30219	5,7,11,14	RW LMi	1641	1403	10 13 11.0	+30 49 17	2
-10236	4,8,10,11,14	IY Hya		1406	10 14 34.4	-14 24 31	2
-30165	5,7,10	CZ Hya	1681	4781S	10 24 56.9	-25 17 39	2
-10242	2,5,6,7	U Hya	1714	1427	10 35 4.97	-13 7 26.2	1
+70100	2,3,5,7,11,13	VY UMa	1736	1433	10 41 37.14	+67 40 27.3	1
-20218	2,5,7	V Hya	1766	1439	10 49 11.30	-20 59 4.9	1
00217	2,5,7,10	SS Vir	1999	1549	12 22 40.7	+1 2 48	2
+50219	2,3,5,6,7	Y CVn	2030	1576	12 42 47.08	+45 42 47.9	1
00224	2,3,5,7,10,14	RU Vir	2032	1579	12 44 45.7	+4 25 4	2
+70116	2,3,5,7	RY Dra	2047	1588	12 54 28.10	+66 15 52.0	1
+40273	2,3,5,7	V CrB	2293	5311	15 47 44.08	+39 43 22.7	1
-10339	2,5,7,11	V Oph	2334	1859	16 23 56.58	-12 18 54.7	1
-30268	5,7	SU Sco	2353	1878	16 37 25.27	-32 17 1.1	1
-30277	5,7,10	V901 Sco	2388		16 59 30.6	-32 39 19	2
-30293	7,9,10	V522 Oph	2438	1961	17 20 50.0	-29 16 44	2
-20364	2,5,7,10	TW Oph	2449	1971	17 26 46.5	-19 26 4	2
-20382	2,4,5,7	SZ Sgr	2478	5134S	17 42 00.17	-18 38 14.0	1
-30333	5,7,10	V781 Sgr	2499	5156S	17 52 48.0	-28 1 25	2
+60255	3,5,7	T Dra	2512	2040	17 55 37.4	+58 13 24	2
-20420	4,7,9,10		2521	5181S	17 59 31.4	-19 10 27	2
-10396	11,14	FX Ser		2067	18 4 4.8	-9 41 42	2
-10397	4,7,9,10		2530	5197S	18 4 10.9	-14 36 3	2
-30364	7,10		2535	2076	18 6 11.0	-27 39 12	2
-30365	5,7,10	V1280 Sgr	2540	2082	18 7 20.2	-26 52 36	2
-10409	4,5,7	ES Ser	2563	2114	18 15 31.8	-13 27 33	2
-20464	2,4,5,7	FO Ser	2567		18 16 29.44	-15 38 4.6	1
-20482	9,10	V2548 Sgr		2151	18 23 27.8	-22 6 4	2
00351	3,7,10		2586	2158	18 24 25.2	+1 7 10	2
-20488	2,4,5,7,10	SS Sgr	2595		18 27 32.1	-16 55 56	2
00353	2,3,4,5,7	TY Oph	2602	2180	18 28 54.4	+4 20 43	2
-10433	10			2182	18 29 51.90	-14 54 12.5	1
+40321	2,3,5,7	T Lyr	2608	2187	18 30 36.19	+36 57 38.9	1
-10441	2,4,5,7,9	RX Sct	2620	2203	18 34 21.4	-7 38 47	2
+20370	14,16,17	NSV 11225		2232	18 39 41.6	+17 38 11	2
00365	4,7,14	NSV 11233	2642	2233	18 39 48.3	-2 20 24	2
+40325	2,3,5,7	HK Lyr	2651	2240	18 41 5.6	+36 54 28	2
-20518	5,7,10	NR Sgr	2657		18 44 29.7	-24 0 15	2
+10379	3,4,5,7	DR Ser	2661	5295S	18 44 53.4	+5 23 59	2
-10467	2,4,5,7	S Sct	2666	2260	18 47 37.09	-7 57 59.4	1
-10469	4,5,7,10	AI Sct	2669	2262S	18 48 10.7	-6 47 57	2
-10475	2,4,5,7,10	T Sct	2678	5324S	18 52 44.3	-8 15 5	2
00402	3,10			2288	18 55 55.6	+4 35 49	2
+10389	2,3,4,5,7	UV Aql	2684	2292	18 56 15.3	+14 17 40	2
00404	4,5,7,9	VX Aql	2687		18 57 33.8	-1 39 13	2
+10397	4,7		2692		18 59 52.9	+10 10 04	2
+10401	4,7,14	NSV 11689	2694	2310	19 0 53.0	+7 26 19	2
-10486	2,5,6,7	V Aql	2695	2314	19 1 43.95	-5 45 38.2	1
00418	3				19 12 25.8	-3 23 24	2
+20393	3,4,5,7	CG Vul	2717	2358	19 14 45.9	+21 49 29	2
-20554	2,5,7	V1942 Sgr	2721	2363	19 16 17.82	-16 0 3.0	1
-10502	14	NSV 11912		2368	19 17 35.3	-8 7 49	2
+40345	5,7	U Lyr	2724	5367S	19 18 24.2	+37 46 55	2
+80036	2,3,5,7	UX Dra	2738	2384	19 23 22.41	+76 27 41.7	1
+20406	3,4,7		2733		19 24 55.2	+23 29 52	2
+50295	3,5,7	AW Cyg	2739	2396	19 27 18.0	+45 56 20	2
00438	3,5,7,10	V374 Aql	2737	2400	19 27 40.2	-0 56 30	2
-20568	2,5,7	AQ Sgr	2744	2416	19 31 27.10	-16 29 2.2	1

TABLE 1—*Continued*

TMSS	Spectrum Reference	GCVS/NSV	Case	RAFGL	α (1950)	δ (1950)	Position Reference
+30374	14,16	V1129 Cyg		2417	19 32 8.8	+27 57 30	2
+30382	2,3,5,7	TT Cyg	2773	2432	19 39 1.90	+32 30 2.2	1
+30385	7	IN Cyg	2783	2443	19 41 40.9	+34 22 10	2
+20435	5,7	CU Vul	2798		19 46 24.7	+21 32 33	2
+30392	4,7		2801	5431S	19 46 40.1	+26 0 48	2
+40368	2,3,5,7	AX Cyg	2833	2480	19 55 35.5	+44 7 34	2
+30408	7	V1583 Cyg	2849	5455S	20 0 32.3	+30 38 12	2
+20452	2,3,5,7	X Sge	2853	2504	20 2 52.6	+20 30 19	2
+50316	2,3,5,7	SV Cyg	2872	2516	20 7 58.6	+47 43 25	2
+40389	3,4,5,7	AY Cyg	2870		20 8 0.3	+41 20 42	2
+30416	4,7	NSV 12861	2871	5473S	20 8 17.2	+29 11 13	2
+40391	2,3,4,5,7	RY Cyg	2873		20 8 30.4	+35 47 54	2
+40393	3,4,5,7	V429 Cyg	2874	2519	20 9 13.4	+35 57 51	2
+40397	4,5,7	RS Cyg	2880	2528	20 11 34.54	+38 34 36.4	2
-20585	2,5,7,10	RT Cap	2882	2542	20 14 11.0	-21 28 23	2
+40403	2,3,4,5,7	WX Cyg	2892	5495S	20 16 41.5	+37 17 36	2
+50324	2,3,4,5,7	U Cyg	2894	2556	20 18 3.21	+47 44 9.9	1
+40417	5,7	V1378 Cyg	2904		20 24 53.6	+38 03 51	2
+40436	3,4,7		2918	5526S	20 35 40.8	+36 40 9	2
+50338	2,3,4,5,7	V Cyg	2923	2632	20 39 41.32	+47 57 45.4	1
+30447	3,5,7	V569 Cyg	2924		20 41 30.2	+31 56 31	2
+30456	3,7		2935	5547S	20 47 14.9	+33 2 36	2
+50346	2,3,5,7	DS Cyg	2937		20 48 37.5	+45 13 45	2
00499	5,7,10	RV Aqr	2968	2702	21 3 17.7	-0 24 43	2
+50357	7,8,12,14,16	V1549 Cyg	2976	2704	21 3 32.6	+51 36 18	2
+40478	3,4,5,7	YY Cyg	3025	2755	21 20 33.5	+42 10 56	2
+70170	3,5,7	AX Cep	3035	2768	21 26 14.7	+70 0 9	2
+40484	3,4,7	V624 Cyg	3040		21 31 19.3	+43 41 51	2
+40485	3,5,7,8,11,14	V1426 Cyg	3041	2781	21 32 5.9	+38 50 54	2
+60321	2,3,5,7	LU Cep	3045	5627S	21 33 51.3	+60 40 48	2
+80048	2,3,5,7	S Cep	3055	2785	21 35 52.65	+78 23 58.7	1
+70172	1				21 38 09.8	+65 33 01.2	2
+50388	4,5,7,14	V644 Cyg	3054		21 38 17.8	+45 13 39	2
+50389	3,7	V1617 Cyg	3058	2791S	21 38 48.3	+51 30 58	2
+40489	2,3,5,6,7	V460 Cyg	3060	2793	21 39 54.35	+35 16 53.3	1
+40491	2,3,5,7	RV Cyg	3063	2798	21 41 12.01	+37 47 16.9	1
+70177	3,7	PQ Cep	3070	2805	21 44 1.2	+73 24 11	2
+50399	3,4,5,7	LQ Cyg	3069		21 44 52.7	+52 20 9	2
+50403	4,5,7	V1398 Cyg	3076		21 50 5.5	+54 51 7	2
+50408	3,4,5,7	V413 Cyg	3081	2816	21 53 20.0	+54 14 46	2
+50409	2,3,4,5,7	LW Cyg	3080	2817	21 53 22.1	+50 15 35	2
+20523	2,3,5,7	RX Peg	3082	2818	21 54 03.1	+22 37 28	2
+30484	5,7	RZ Peg	3107		22 3 40.4	+33 15 48	2
+50418	3,4,5,7	CT Lac	3111	5670S	22 4 41.9	+48 12 28	2
+60358	4,7		3140		22 30 33.9	+58 21 39	2
+60365	2,3,4,5,7	DG Cep	3152	2948	22 42 17.7	+61 27 58	2
+50455	3,5,7	VY And	3174	3015	22 59 33.3	+45 37 0	2
+60393	15	NSV 14477		3056	23 13 53.4	+62 4 57	2
+60403	3,5,7	V353 Cas	3186	5764S	23 21 10.5	+55 53 33	2
+60409	15	V582 Cas		3109	23 27 53.0	+60 00 14	2
+60411	15	V530 Cas		4299	23 28 25.7	+59 58 49	2
+60412	3,4,5,7	DS Cas	3190		23 30 2.5	+61 49 58	2
+40540	11,14	NSV 14623		3116	23 32 1.3	+43 16 27	2
00532	2,3,5,6,7	TX Psc	3202	3147	23 43 50.10	+3 12 33.7	1
+60433	2,4,5,7	WZ Cas	3214	3196	23 58 41.89	+60 4 37.4	1

SPECTRAL CLASSIFICATION REFERENCES.—(1) Bidelman 1980. (2) *Henry Draper Catalogue* (Cannon and Pickering 1918–1924). (3) *Dearborn Catalogue of Faint Red Stars* (Lee *et al.* 1947). (4) The Case Objective Prism Survey: Nassau and Blanco 1954*a*, *b*; Nassau, Blanco, and Morgan 1954; Nassau, Blanco, and Cameron 1956; Nassau and Blanco 1957; Blanco and Nassau 1957. (5) *General Catalogue of Variable Stars* (Kukarkin *et al.* 1969–1971). (6) *Bright Star Catalogue* (Hoffleit and Jaschek 1982). (7) Baumert 1974. (8) Dyck, Lockwood, and Capps 1974. (9) Hansen and Blanco 1973. (10) Hansen and Blanco 1975. (11) Lockwood 1974. (12) Lockwood and McMillan 1971. (13) Lockwood and Zinter 1973. (14) Merrill and Stein 1976. (15) Poulakos 1978. (16) Vogt 1973. (17) Wyckoff and Wehinger 1974.

POSITION REFERENCES.—(1) *SAO Catalog*. (2) This paper. (3) Becklin *et al.* 1969.

positions were measured either at the 1.3 m telescope at Kitt Peak National Observatory or on the POSS plates with the Grant measuring engine at NOAO; they have estimated uncertainties $\pm 3''$ in each coordinate.

The much smaller number of carbon stars seen in the TMSS, compared with those detected in the Case survey (Stephenson 1973), results from the fact that the TMSS samples a smaller volume of space. Examination of stars lying at $b > +30°$ shows that the fraction of Case carbon stars detected by the TMSS is significantly greater for N-type carbon stars than for the R-type stars. The implications of this difference, in terms of the luminosities of the two groups, are reviewed in § VI.

The TMSS found 24 carbon stars which had not been detected in the Case objective-prism survey (Stephenson 1973). Of these, 15 fell in the region of the sky covered by both surveys. At least three causes for the nondetection of these stars in the Case survey can be readily identified. First, a few stars, such as TMSS +10216, are extremely red (*observed* $I' - K > 6$ mag). Second, these and other stars missed by the Case survey are known infrared variables. Third, a few stars are located near other bright optical objects, and may have been lost as a result of confusion in the Case survey.

Only 159 of the sources in Table 1 were detected in the AFGL survey. However, 37 carbon stars were found in the AFGL survey but were not seen in the TMSS (Kleinmann, Gillett, and Joyce 1981). These stars are in general much redder than those detected in the TMSS, and represent a group of carbon stars that is undersampled by near-infrared surveys. The impact of this effect on our assessment of the density of carbon stars is discussed in § VI.

III. SUMMARY OF PHOTOMETRY

The photometric properties of the sample are summarized in Table 2. All measurements were placed on the standard photometric systems defined by Johnson (1965), and were corrected for interstellar reddening as discussed below. The suffix "v" on an entry indicates that the source is thought to be variable at that wavelength (§ IV). The TMSS I'-magnitudes were converted to the standard photometric I band using the relation (Payne-Gaposchkin and Whitney 1976)

$$I - K = 0.745(I' - K) - 0.13.$$

The photometric survey by Noguchi *et al.* (1981) provided $J'H'K'$ magnitudes for 123 stars of the objects in our sample. We converted them to J (1.25 μm), H (1.65 μm), and K (2.2 μm) magnitudes in the Johnson system using the following relations, derived by comparing photometry obtained by Noguchi *et al.* (1981) with that of Bergeat and Lunel (1980):

$$J = J' - 0.14(J' - K') + 0.56,$$

$$H = H' - 0.007(J' - K') + 0.24,$$

$$K = K' - 0.034(J' - K') + 0.20.$$

The J, H, and K data from Noguchi *et al.* (1981) and the TMSS I and K data were corrected for interstellar extinction using an iterative method similar to that outlined by Cohen *et al.* (1981). The compilation of the Galactic reddening distributions by Lucke (1978) were used to determine the reddening gradient for each line of sight, and the reddening law given in Cohen *et al.* (1981) was used to obtain the color excesses at wavelengths of interest. The total extinction and distances to each carbon star in our sample were computed by assuming (see below) that they all had the same luminosity at 2.2 μm, $M(K) = -8.1$.[2] The 2.2 μm extinction (A_K) derived by this method is listed along with the corrected photometry in Table 2.

Photometry at 4.2 μm was obtained from the RAFGL catalog (Price and Murdock 1983) for 150 sources, and at longer wavelengths from the *IRAS* survey for 210 sources. (Five stars in our sample, TMSS −20199, −10236, −10441, +50346, and +20523, were in regions of the sky not included in the *IRAS* survey.) Photometry from the PSC was used for all but the 89 objects listed in the PSC with $F(60\ \mu\text{m}) < 2.5$ Jy. For these stars, improved signal-to-noise (especially at the longest wavelengths) was obtained by co-additions of all available *IRAS* survey data. To do this, we used the "Add-Scan" program at IPAC,[3] and adopted the peak flux density of the median scan across each source as the true flux density of the source. These values were systematically higher by an average of 5% in the 12 μm band and 10% in the 25 μm band than the flux densities listed in the PSC.

All of the *IRAS* photometry was color-corrected according to the method described by Hacking *et al.* (1985). The data were than converted to magnitudes using the calibration specified in the *IRAS Catalogs and Atlases Explanatory Supplement* (1985). Sources with detections weaker than 5 σ in the Add-Scan photometry are indicated by a colon following the value; 3 σ upper limits are given for bands in which the sources were not detected.

IV. TEMPORAL PROPERTIES

The great majority (194, or 90%) of the stars in our sample are known or suspected variables. All but one of these are identified with named or suspected variables, listed in Kukarkin *et al.* (1969–1971, hereafter GCVS) and its supplements. Of these, 96 were found to be semiregular or Mira-type variables, whose periods range from 60 to 640 days. Information on the infrared variability of these objects is also available from both the TMSS and *IRAS* survey data. Sources are noted in Table 2 as potentially variable at I or K, if the dispersion of the measurements was larger than that which should be statistically exceeded only 10% of the time. Sources are listed as variable at 12 or 25 μm in Table 2 if the PSC indicates a probability > 50% that the source varied at one of these wavelengths during the course of the *IRAS* survey.

[2] This value is the average for 54 carbon stars observed in the Magellanic Clouds by Cohen *et al.* (1981) and Frogel, Persson, and Cohen (1980), assuming distance moduli of 18.6 and 19.1 for the LMC and SMC, respectively. For these stars, the dispersion about the average is ~ 0.6 mag.

[3] IPAC is funded by the National Aeronautics and Space Administration as part of the Extended Mission Program under contract to JPL.

TABLE 2

INFRARED PHOTOMETRY OF CARBON STARS[a]

TMSS	I_o	K_o	J	H	K	A(K)	m[4.2]	m[12]	m[25]	m[60]	m[100]	TMSS	I_o	K_o	J	H	K	A(K)	m[4.2]	m[12]	m[25]	m[60]	n[100]
+40003	4.26	2.18	3.33	2.56	2.21	0.12		1.29	0.94	0.32	-1.11	+30110	4.38	1.99v	3.17	2.38	1.60	0.14	1.3	-0.67v	-1.04v	-1.20	>-2.49
+70003	4.91v	2.49v	3.42	2.52	1.84	0.21	1.1	0.07	-0.16	-0.86	>-3.80	+30114	5.92	1.86v	3.94	2.69	1.52	0.11	-0.1	-1.52v	-1.65v	-2.15	-3.55
+40006	3.52v	0.84	2.21	1.28	0.65	0.07	0.1	-0.36	-0.61	-1.13	-1.57	+10089	4.40v	1.77	2.72	1.89	1.39	0.05		0.49	0.14	-0.46	>-3.27
+40010	4.26v	1.57	2.65	1.87	1.38	0.07	1.0	0.42	0.10	-1.20	-2.47	-30046	4.82	2.65	3.64	2.97	2.48	0.02	1.8	1.80	1.66	1.32	-0.29:
+70009	4.90	2.48				0.20	1.2	1.46	1.18	0.80	>-1.37	+20115	5.83	2.79				0.38		1.42	1.08	0.43	>-3.31
+60026	4.93v	2.44	3.30	2.64	2.30	0.18	2.0	1.45	1.04	0.32	-2.74	+70064	4.69v	2.68	3.82	3.03	2.41	0.12		1.84v	1.47v	1.52	>-0.92
+60034	4.82	2.73	4.08	3.19	2.74	0.24	1.4	1.73	1.30	-0.39	-2.52	-10095	6.59	2.65v				0.05	0.7	0.21	0.01	-0.35	>-4.92
+50030	6.08	2.19v	4.23	2.91	1.83	0.13	0.8	-0.69	-1.07	-1.28	>-2.19	+10094	4.32v	1.90				0.21	0.5	-0.01	-0.32	-0.68	-1.92
+60041	4.51	1.57v	5.10	3.57	2.31	0.13	0.0	-1.42	-1.63	-1.90	>-3.73	+20120	4.19	1.67	2.96	2.05	1.46	0.09	0.8	0.12	-0.05	-0.60	>-1.76
+30025	3.29	0.78	1.85	1.03	0.63	0.02	0.3	0.09	-0.29	-0.92	-1.40	+20121	2.95	0.34	1.52	0.64	0.18	0.05	-0.4	-1.51	-1.91	-2.33	-2.35
-30015	2.65v	0.03	0.55	-0.14	-0.61	0.00	-0.9	-1.75	-2.56	-3.99	-4.22	+40140	6.21	2.76	6.44	5.11	3.65	0.20	0.8	-0.45v	-1.32v	-1.27	-1.24
+60056	4.95	2.38	3.74	2.78	2.18	0.15		0.98	0.68	0.36	>-1.75	+30127	3.76	2.02	2.95	2.18	1.77	0.12		1.05	0.65	0.03	>-1.33
+60069	5.02	2.31	3.67	2.77	2.17	0.15	1.7	0.82	0.54	0.21	>-3.04	+40141	4.95	2.68	4.05	3.34	2.72	0.20		1.68	1.40	0.57	-0.54:
+50061	4.79	2.52	4.09	3.16	2.58	0.15		1.38	1.09	0.28	-2.04	-10104	5.03	2.36				0.03	1.5	1.85	1.73	1.69	>-2.82
-30021	5.21	1.30				0.00	-0.8	-2.08	-2.30	-2.52	-2.54	+40151	5.57v	2.49	4.77	3.71	2.66	0.11	1.2	-0.29v	-0.51v	-0.85	>-1.51
+60113	3.51	1.23	2.05	1.31	0.90	0.12	0.2	1.30	-0.24	-0.65	>-3.67	+30143	3.51	0.93	1.78	0.94	0.51	0.07		-0.68	-0.92	-1.47	-2.17
+50088	4.32	2.28	3.35	2.64	2.31	0.20		1.31	1.05	0.54	>-1.22	+10113	5.03	2.10	3.92	2.88	2.13	0.07	1.2	0.82	0.52	-0.12	-1.76
+50096	5.93	2.01v	4.10	2.51	1.03	0.17	-0.9	-2.96v	-3.36v	-3.69	-3.58	+10118	5.71	2.33	3.98	2.93	2.16	0.07	1.3	0.33	-0.07	-0.91	-1.68
+60124	3.03	0.30	1.89	0.94	0.29	0.08	-0.6	-1.31	-1.73	-2.68	-2.98	00103	4.23	1.53				0.05	1.1	0.85	0.57	-0.41	-2.48
+50100	3.74	0.91	2.47	1.56	0.88	0.10	0.3	-0.42	-0.77	-1.70	-3.03	+30150	4.94v	2.81	4.17	3.37	2.66	0.15		1.52v	1.32v	0.95	>-3.78
+40067	4.73	2.19	3.22	2.51	1.95	0.19		0.76	0.51	0.20	>-2.75	+10119	5.52	2.87	4.07	3.36	3.02	0.09		1.27	1.07	0.55	>-0.76
+40070	5.75	2.24v				0.21	0.6	-1.40	-1.57	-1.83	-1.63	-30060	4.89	2.38				0.03		0.61	0.29	-0.29	-1.30
+60138	3.87	2.03	2.62	2.07	1.84	0.17	1.2	1.32	1.19	0.98	>-1.19	+10121	2.84	0.67	1.59	0.83	0.49	0.08	0.1	-0.21	-0.52	-1.16	-2.01
+30074	4.94	2.25	3.03	2.47	2.14	0.22		1.19	0.47	0.30	>-3.28	-10122	5.68v	2.58				0.06	0.3	-1.33v	-1.63v	-2.06	-2.70
+50115	4.39	1.78				0.17	0.6	1.11	0.41	0.07	-1.69	+20145	4.52	2.36				0.19	1.5	0.87	0.50	-0.27	-2.06
+40089	4.54	1.47				0.16	1.0	-0.24	-0.55	-1.13	-1.82	+40157	4.87	2.81				0.13		1.75	1.52	0.45	-0.40:
+70055	2.74	0.35	1.47	0.60	0.20	0.07	-0.4	-0.98	-1.18	-1.67	-2.56	+20152	4.20	1.34				0.11	0.8	-0.16	-0.67	-0.95	>-3.25
+20094	4.19	2.49				0.27		0.96	0.69	0.55	>-1.76	+40158	1.72v	-0.73	0.69	-0.22	-0.68	0.05	-1.3	-1.99	-2.27	-2.80	-3.34
+30098	3.26	0.90	1.98	1.22	0.76	0.15	0.2	0.11	-0.31	-1.74	-2.46	-10133	5.69	2.81				0.08		1.56	1.34	1.25	>-0.91
+40101	3.92	1.42				0.15	1.6	0.74	0.08	-0.56	>-3.24	+30163	4.60	2.52	3.27	2.56	2.19	0.11		1.40	1.18	0.79	>-0.69
+50130	6.03	2.57				0.23	1.6	0.76v	0.51v	0.15	>-1.45	00123	5.42	2.83				0.08		2.17v	1.97v	1.53	>-0.45
+20095	4.42	2.53				0.29		1.52	1.25	0.59	>-1.26	-20101	5.07	2.47				0.20	0.9	0.37	-0.32	-1.59	-1.74
-10080	3.62v	0.05v	2.39,	0.73	0.11	0.01	-1.6	-2.52v	-2.79v	-3.09	-3.20	00125	5.20	2.67	4.15	3.12	2.46	0.09		1.09	0.79	0.08	-1.37:
+50135	4.33	1.45				0.09	0.7	0.09	-0.26	-0.89	-1.97	00127	5.69	2.85	4.51	3.51	2.80	0.09	1.5	1.64	1.24	-0.22	-3.25:
00066	2.08	-0.37	1.13	0.22	-0.32	0.03	-1.2	-1.70	-1.92	-2.48	-2.80	00131	5.66	2.73v	6.68	5.02	3.52	0.08	0.8	-0.21v	-0.78v	-1.03	>-3.44
+40115	4.48	2.11	3.28	2.62	2.07	0.17		0.76	0.47	-0.01	-1.39	00136	4.77	2.32	3.32	2.47	2.09	0.03		1.19	0.88	0.36	-2.00
-10083	4.77	2.35	3.38	2.59	2.10	0.07		1.08	0.67	0.14	-0.60:	+10144	5.26	1.75	4.01	2.68	1.56	0.05	0.3	-1.15	-1.31	-1.70	-1.68
+10081	4.58v	1.75				0.09	0.6	0.07	-0.20	-0.94	>-3.04	+10146	4.15v	1.88	2.25	1.46	1.06	0.05	0.7	0.24	0.05	-0.30	>-1.11
+40120	4.36	2.45	3.14	2.58	2.21	0.25	1.4	1.48	1.17	0.91	>-2.09	00141	4.32	1.97	3.03	2.23	1.80	0.02	1.0	0.88	0.72	-0.32	-3.10:
+10083	4.72	2.08				0.18		1.01	0.74	-0.49	>-2.96	-10149	3.75v	1.07	2.33	1.35	0.71	0.02	0.2	-0.48	-0.73	-1.30	>-4.09

TABLE 2—*Continued*

TMSS	I_o	K_o	J	H	K	A(K)	m[4.2]	m[12]	m[25]	m[60]	m[100]
-10152	3.31	0.99	1.91	1.16	0.82	0.03	0.3	-0.16	-0.67	-0.89	>-4.37
+10154	5.55	2.85	3.61	2.80	2.25	0.07	1.7	1.04v	0.81v	0.09	-2.05
+10156	5.80v	2.87v	4.04	3.23	2.66	0.07	1.7	1.32v	1.11v	0.66	>-0.05
+10158	5.55	2.75	4.19	3.22	2.50	0.07	1.6	1.31	1.07	0.57	>-0.74
+30182	4.68	2.79	3.77	3.02	2.58	0.16		-0.12	-1.09	-0.82	-1.08
-20131	6.90	2.66	4.71	3.40	2.22	0.04	0.7	-0.99	-1.26	-1.33	>-3.88
00158	5.40	2.79				0.04		1.67	1.34	0.26	-0.99
-30097	5.16	2.23				0.02	1.1	0.14	-0.22	-0.74	>-3.14
-10177	5.68	2.79	4.56	3.59	2.83	0.02		1.71	1.42	0.95	0.49:
00162	6.36	2.77v	5.56	4.32	2.96	0.03	0.9	-0.21v	-0.51v	-0.71	-1.19
-30106	4.97	2.63				0.03		0.88	0.03	-0.08	>-1.74
-30114	5.24	2.27				0.03	1.3	0.53	-0.17	-0.38	-1.46
-20156	4.62	1.94				0.02	1.5	0.49	0.19	-0.31	>-0.84
00172	5.30v	2.13	4.10	3.12	2.34	0.01	0.9	0.18	-0.03	-0.32	-0.83
-20165	5.60	2.68	4.08	3.18	2.60	0.03		1.47	1.27	1.07	>-0.16
-30132	5.71	2.37				0.10		-0.84	-1.30	-1.47	-1.68
-30133	5.98	2.71				0.05		0.61	0.26	0.04	>-0.50
-30134	3.90	1.75	3.02	2.17	1.75	0.03		0.67	0.44	-0.41	-1.83
+20206	2.66	0.13	1.88	0.86	0.23	0.00	-0.5	-0.93v	-1.16v	-1.72	-2.10
+20207	4.59v	1.35	2.66	1.63	0.93	0.01	0.0	-0.49	-0.66	-0.99	-1.22
-20184	5.48	2.42				0.03		0.09v	-0.12v	-0.58	-1.11
+10216	5.71	1.30v				0.01	-3.5	-7.91v	-8.57v	-9.08	-8.31
-20199	3.15	0.54				0.10					
+30219	6.64	1.15v				0.00	0.3	-2.32	-3.65	-4.40	-5.73
-10236	6.34	2.61				0.20	-1.0				
-30165	6.61v	2.76v				0.04	1.0	-0.44	-0.85	-1.04	-1.56
-10242	1.58	-0.69	0.41	-0.47	-0.84	0.04	-1.4	-1.90	-2.28	-2.76	-3.76
+70100	2.82	0.53	1.67	0.81	0.40	0.03	0.1	-0.31	-0.53	-1.41	-2.59
-20218	2.68v	-0.42v	1.49	0.20	-0.67	0.02	0.5	-3.78	-4.29	-4.62	-4.53
00217	3.26	0.73v	2.42	1.44	0.68	0.00	-0.1	-0.99	-1.25	-1.40	-1.40
+50219	1.72v	-0.78	0.56	-0.39	-0.92	0.01	-1.4	-2.10	-2.24	-2.68	-3.04
00224	5.63v	1.92v	3.61	2.48	1.32	0.01	0.2	-1.97	-2.20	-2.48	-2.30
+70116	2.95	0.24v	1.23	0.46	-0.01	0.03	-0.6	-1.14	-1.37	-1.89	-2.38
+40273	5.24v	1.92v	2.92	1.93	1.14	0.05	0.5	-1.13v	-1.37v	-1.52	-1.56
-10339	3.99v	1.48	2.21	1.66	1.15	0.23	0.9	0.22	0.00	-0.45	-0.30:
-30268	3.67v	1.03	2.36	1.38	0.71	0.13	0.5	-0.15v	-0.45v	-1.00	>-2.49
-30277	4.77v	2.60				0.21		1.04	0.83	0.05	-2.33
-30293	4.38	1.69				0.14	1.1	0.18	0.00	>-0.59	>-4.52
-20364	3.07	0.19				0.07	-0.3	-0.98	-1.16	-1.63	>-2.37
-20382	4.22	1.91				0.14	1.4	0.57	-0.18	-0.57	>-2.64
-30333	5.24	1.97				0.12	1.7	0.69	0.45	>-3.09	>-6.95
+60255	4.98	1.09	4.55	3.05	1.73	0.02	-0.4	-1.84v	-2.18v	-2.54	-2.67
-20420	5.05	2.53				0.17	1.8	0.08	-0.68	>-1.21	>-4.38
-10396	6.92	2.25v				0.19	0.2	-1.98v	-2.47v	-2.83	>-3.28
-10397	4.99	2.71				0.27	1.4	1.16	0.98	>-1.98	>-5.88
-30364	4.07	2.25				0.40	0.3	-0.60	-0.94	-1.15	>-5.74
-30365	5.51	2.25v				0.13	1.2	-0.97v	-1.27v	-1.61	>-5.55
-10409	4.04	1.53				0.17	1.0	-0.08	-0.35	>-3.78	>-7.41
-20464	4.36	2.60				0.23		1.40	0.46	>-3.38	>-5.53
-20482	4.84	2.21				0.70	0.6	-1.08	-2.13	-2.87	>-4.66
00351	5.56	2.05	3.61	2.55	1.92	0.20	1.1	0.48	0.17	-0.47	>-2.71
-20488	4.17v	2.35				0.23		1.32	0.89	-0.39	>-4.33
00353	4.42	1.66	3.23	2.22	1.68	0.14	1.0	0.48	0.11	-0.55	-2.99
-10433	2.20	0.89				0.13	0.9	0.61	0.49	-0.38:	-3.65:
+40321	3.52	0.43	2.08	0.97	0.17	0.02	-0.5	-1.02	-1.34	-1.50	-1.87
-10441	4.86	1.74				0.65	1.0				
+20370	4.85	1.88v	5.03	3.27	1.78	0.13	-1.7	-3.01v	-3.61v	-4.00	-4.09
00365	5.25	2.43v				0.24	-0.9	-3.06v	-3.61v	-3.83	>-5.21
+40325	4.34	1.65	3.13	2.14	1.60	0.04	0.9	0.53	0.23	-0.45	-1.35
-20518	5.18	2.54				0.15		1.23	1.00	0.40	-1.11:
+10379	4.61	1.86	3.43	2.42	1.86	0.13	1.3	0.82	0.15	-1.62	>-3.31
-10467	2.85	0.47	1.73	0.91	0.35	0.09	-0.1	-0.55	-0.81	-2.17	-3.78
-10469	4.79	2.57				0.30	1.9	0.65v	0.42v	-0.80	>-5.58
-10475	4.42	2.49				0.29	1.3	1.77	1.42	0.96	>-0.05
00402	4.86	1.51	2.80	1.83	1.36	0.14	0.9	-1.10	-1.90	-2.91	>-6.69
+10389	4.01v	1.59v	2.76	1.83	1.34	0.14	1.0	0.41	0.13	-0.65	>-3.28
00404	5.25v	2.56v				0.22		0.70v	0.25v	-0.40:	>-3.25
+10397	4.57	1.98	3.16	2.28	1.91	0.18		1.14	0.63	-0.19	>-2.85
+10401	7.34	2.57v	5.49	3.68	2.32	0.23	-0.5	-2.80	-3.27	-3.46	>-6.30
-10486	2.39	-0.17	1.31	0.36	-0.27	0.08	-0.9	-1.44	-1.59	-2.26	-2.73
00418	3.89	2.71				0.27		2.36	2.03	>1.18	>-3.53
+20393	4.51	1.60	3.33	2.24	1.66	0.10	0.7	0.34	0.06	-0.66	>-2.23
-20554	3.92	2.51	1.38	0.90	0.67	0.29	0.29	0.8	0.06	-1.16	-2.88
-10502	5.46	1.72v				0.18	-0.8	-2.69v	-3.38v	-3.74	-3.79
+40345	4.81	2.12	3.73	2.90	2.12	0.08	1.0	0.36	0.16	-0.25	>-0.67
+80036	2.58	0.08				0.02	-0.1	-0.62	-0.85	-1.36	-2.30
+20406	5.31	2.65	4.22	3.20	2.59	0.15		1.02	0.77	0.66	>-2.81
+50295	4.44	1.89	3.27	2.37	1.80	0.11	1.1	0.57	0.28	-0.57	-1.43
00438	6.18	2.47v				0.20	0.5	-0.49v	-1.03v	-1.34	>-1.34
-20568	3.14	0.61				0.09	0.1	-0.48	-0.85	-1.58	-2.79

TABLE 2—*Continued*

TMSS	I_o	K_o	J	H	K	A(K)	m[4.2]	m[12]	m[25]	m[60]	m[100]
+30374	5.84	2.69v	5.11	3.34	1.87	0.11	-0.4	-2.52v	-3.23v	-3.52	-3.64
+30382	3.97	1.82	3.17	2.28	1.81	0.08	1.0	0.99	0.69	-1.11	-2.50
+30385	6.28	2.74	5.48	4.06	2.99	0.16	1.2	-0.43v	-0.69v	-0.68	>-3.48
+20435	5.45	2.55	4.38	3.53	2.78	0.15		1.13v	0.85v	0.79	>-4.76
+30392	5.85	2.65	4.16	3.09	2.55	0.15	1.5	1.34	0.96	>-0.98	>-4.67
+40368	3.87v	1.22	2.99	1.94	1.35	0.08	0.7	0.10	-0.12	-0.77	>-4.74
+30408	5.08	2.74	4.05	3.30	2.64	0.16	1.7	1.45	1.25	>-0.85	>-4.92
+20452	4.47	1.82	3.15	2.36	1.74	0.08	1.0	0.82	0.38	-0.57	-1.87
+50316	4.30	1.78				0.12	1.2	0.77	0.41	-0.30	>-2.11
+40389	5.26	2.72				0.18		1.55	0.79	>-1.32	>-4.34
+30416	6.24	2.85v	6.56	4.89	3.43	0.15		0.21v	-0.05v	-0.34	>-4.87
+40391	4.47	2.36	3.74	3.01	2.48	0.14		1.61	1.43	>-1.36	-3.52:
+40393	4.83	2.17	3.83	3.25	2.95	0.13	1.1	1.16	>0.87	>-1.34	>-5.17
+40397	3.31	1.02	2.19	1.56	1.09	0.08	0.6	0.41v	0.00v	-0.81	>-5.37
-20585	3.05	0.47				0.03	0.0	-0.70	-0.90	-1.26	-2.24
+40403	5.16	2.08	3.63	2.88	2.12	0.12	1.5	1.27v	0.99v	>-2.62	>-6.14
+50324	4.50	1.50	2.94	2.08	1.20	0.10	0.4	-1.22v	-1.51v	-1.86	>-3.91
+40417	4.58	2.14				0.60		1.68	1.48	>-2.99	>-6.08
+40436	5.35	2.17	3.82	2.72	2.10	0.13	1.2	0.88	0.44	>-0.27	>-6.44
+50338	4.87v	0.72v				0.08	-1.9	-3.17	-3.54	-3.77	-3.91
+30447	5.14	2.73	3.94	3.06	2.60	0.17		1.50	1.20	0.04	-2.28
+30456	5.09	2.36	3.57	2.70	2.27	0.14	1.1	0.83	0.48	-0.85	-2.31
+50346	6.39	2.67				0.45					
00499	5.79v	1.43v				0.03	-0.6	-2.36v	-2.77v	-2.93	-3.13
+50357	7.51	2.97v	5.59	3.78	2.44	0.23	1.2	-2.19v	-2.72v	-2.88	>-4.85
+40478	5.08	2.46				0.14	1.0	1.36	1.08	0.41	-2.63
+70170	5.78	2.24v				0.16	0.5	-0.62	-1.02	-1.43	-2.32
+40484	5.63	2.47	4.17	3.12	2.53	0.13		1.35	1.06	0.02	-2.71
+40485	6.51	1.94v	3.96	2.35	1.17	0.06	-0.2	-2.16	-2.56	-2.87	-3.28
+60321	4.67	2.64				0.26	1.6	1.64	1.21	-0.01	>-0.40
+80048	3.52	-0.13				0.04	-1.6	-2.57	-2.93	-3.24	-3.57
+70172	5.10	2.75				0.20		1.60	1.28	0.56	>-3.63
+50388	6.41	2.93v				0.18		-0.43	-0.88	-1.29	-1.86
+50389	4.39	1.86				0.14	1.4	0.38	-0.62	-0.26	>-3.78
+40489	2.77	0.27	1.37	0.45	0.05	0.03	-0.4	-0.74	-1.02	-2.06	-2.56
+40491	3.03	0.27	2.01	0.91	0.36	0.03	-0.4	-1.11	-1.43	-2.35	-3.39
+70177	4.54v	1.01v				0.09	-0.5	1.76v	1.36v	0.42	>-1.05
+50399	5.30	2.68				0.22		1.84v	1.44v	0.33	>-3.75
+50403	4.82	2.57				0.23		1.56	1.10	0.17	>-2.06
+50408	4.32	1.93				0.17	1.1	0.73	0.36	-0.63	-3.28
+50409	3.68	1.56				0.14	0.9	0.54v	0.25v	-0.30	>-1.77
+20523	4.94	2.23				0.20	1.2				
+30484	5.95	2.71	3.81	3.18	2.73	0.09		0.74	0.17	-0.08	>-0.38
+50418	4.85	2.23	3.99	3.00	2.39	0.17	1.5	0.40v	-0.10v	-0.72	>-1.94
+60358	5.02	2.45	3.59	2.85	2.27	0.25		1.33	1.06	>-0.43	>-4.53
+60365	3.52	1.61v	2.69	2.00	1.60	0.19	1.2	0.73	0.37	-0.77	>-5.33
+50455	4.60	2.63	3.91	3.27	2.68	0.27	1.6	1.56	1.33	0.58	-1.20
+60393	4.84	1.79v				0.21	1.1	-1.33	-2.22	-2.44	-3.90
+60403	4.56	2.52	3.48	2.90	2.41	0.28	1.8	1.36	1.09	0.28	>-3.53
+60409	4.72	2.42				0.74	0.5	-1.36	-2.39	-2.75	>-4.52
+60411	4.42	1.81				0.19	0.9	-1.62	-2.85	-2.70	-3.77
+60412	4.77	2.52				0.28		1.39	0.86	-2.52	-4.57
+40540	6.48	2.24v				0.16	-0.3	-3.67	-4.33	-4.66	-4.68
00532	1.52	0.74	0.59	-0.37	-0.69	0.02	-1.1	-1.52	-1.64	-2.33	-2.93
+60433	2.93	0.31	1.64	0.84	0.47	0.09		0.1	-0.19	-0.49	-1.03

[a] The magnitudes for the *IRAS* bands were computed assuming zero-magnitude flux densities of 28.3, 6.73, 1.19, and 0.43 Jy for the 12, 25, 60, and 100 μm bands, respectively.

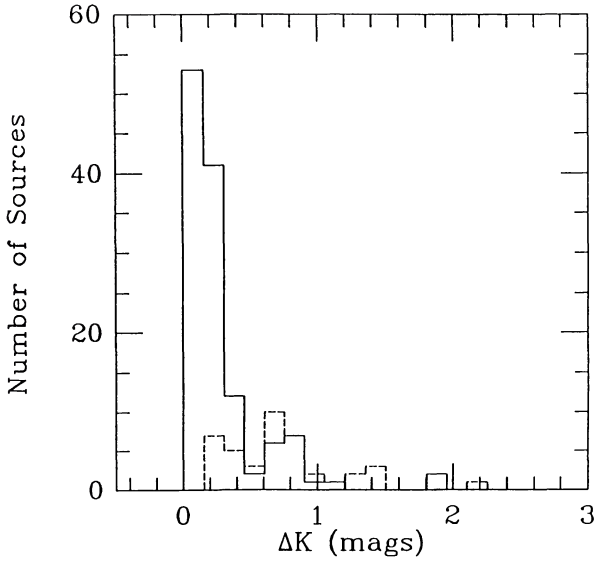

FIG. 1.—*Solid-line histogram*: Absolute value of the difference in K-magnitude between the corrected data of Noguchi *et al.* (1981) and the TMSS for 125 stars which belong to both samples. *Dashed-line histogram*: Absolute value of the maximum difference of the K-magnitude from the individual observations of the TMSS. Note that those stars which showed no χ^2 excess in the TMSS are *not* included in the figure.

From a cross-check on the TMSS and the PSC, we find only one star (TMSS −10122) that was considered to be infrared-variable but was not found in the GCVS.

Two independent estimates of the amplitudes of variability at 2.2 μm for stars in our sample can be made from available photometry. The fact that the TMSS found only 41 out of 215 carbon stars to be variable indicates that few have large (> 0.5 mag) amplitude variations on time scales of months. The distribution of amplitudes of the carbon stars that were found to be variable in the TMSS is shown in Figure 1. The greatest of these is 2.16 mag, which is the amplitude estimated for TMSS +10216. An alternative method for evaluating the amplitudes of infrared variations of carbon stars is to compare the corrected data obtained by Noguchi *et al.* (1981) with the TMSS photometry. Like the data obtained in the TMSS, these K-band differences were measured at random phases in each star's cycle of variations and therefore gives a lower limit to their true amplitudes. A histogram of these differences is shown in Figure 1. It is seen that, consistent with the results of the TMSS photometry, only a few stars differed by more than 0.3 mag, and that the maximum value of the differences is approximately the same as the maximum amplitude determined from the TMSS data.

V. SPECTRAL ENERGY DISTRIBUTIONS

A comparison of the near-infrared colors (J, H, and K) obtained by Noguchi *et al.* (1981) for carbon stars in the TMSS with colors of carbon stars seen in the Magellanic Clouds (Frogel, Persson, and Cohen 1980; Cohen *et al.* 1981) is shown in Figure 2. The carbon stars in the Magellanic Clouds were selected from a near-infrared photographic survey carried out by Blanco, McCarthy, and Blanco (1980), and from surveys at 2.2 and 3.5 μm by Frogel and Richer (1983). It is evident that the majority of carbon stars sampled by the TMSS have near-infrared colors that span the same range as those of the carbon stars seen in the Magellanic Clouds. We also note that most of the carbon stars found in the Magellanic Clouds are, like most of those in the TMSS, of type N (Wood 1985). We infer therefore that the carbon stars in the TMSS have the same average absolute K-magnitude as those found in the Magellanic Clouds.

The distributions in $(I-K)_0$ and $m(K_0)-m(12\ \mu\text{m})$ for our sample are illustrated in Figure 3. The means, standard deviations, and maximum ranges in these colors are summarized in Table 3. By far the reddest star in the sample is TMSS +10216. The broad range in observed $m(K_0)-m(12\ \mu\text{m})$ undermines the assumption of a narrow range in absolute magnitude for carbon stars *both* at 2.2 μm (as in the present paper) and at 12 μm. It is not surprising that these colors vary so much among the carbon stars, since (1) their 12 μm flux densities are, in most cases, dominated by emission from circumstellar dust, and (2) previous studies have shown (Knapp and Morris 1985), and this work confirms (see below), that the masses of circumstellar envelopes of carbon stars range over at least 3 orders of magnitude.

Figure 4 shows the distributions in $(I-K)_0$ and $K_0-m(12\ \mu\text{m})$ for the N stars and R stars separately. These data provide no evidence for color differences between the stars denoted as type N and those denoted type R within our sample. The similarity in the infrared colors of these stars may be attributable to the fact that, as mentioned in § II, the MK classification system indicates a large overlap in the

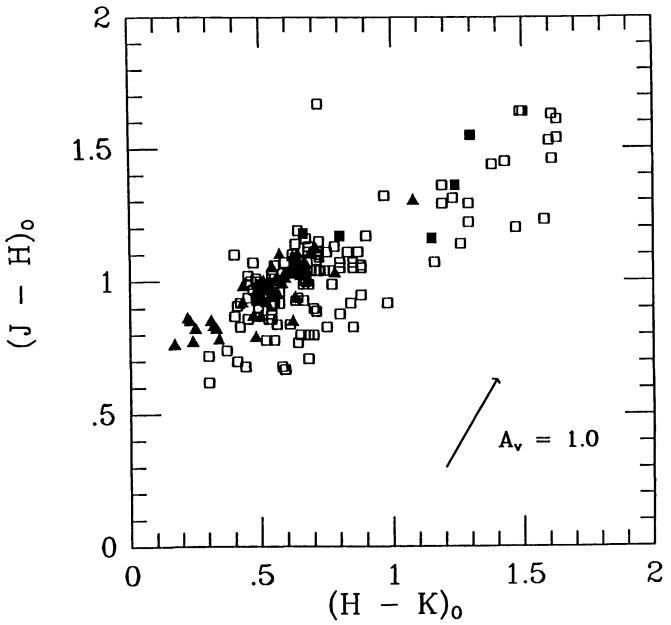

FIG. 2.—$J-H, H-K$ color-color diagram for 125 stars of the TMSS sample (*open squares*), compared with the photometry of Magellanic Cloud carbon stars (*filled triangles*). Filled squares are the colors of carbon stars discovered by Frogel and Richer (1983) in a deep K-band search for red objects in the Bar West field of the LMC.

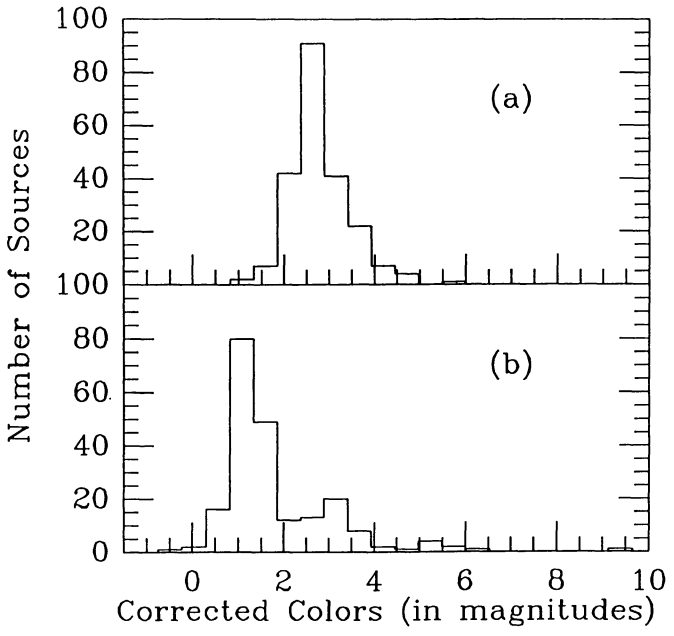

FIG. 3

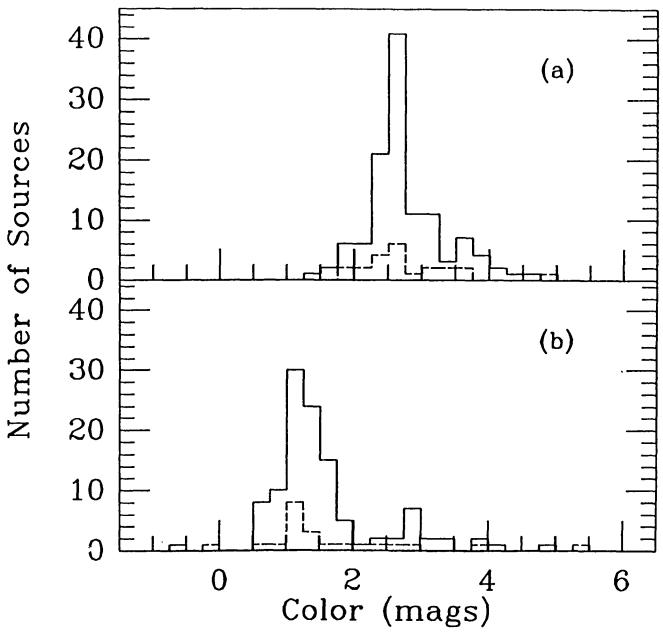

FIG. 4

FIG. 3.—(*a*) Histogram of the $(I-K)_0$ color for the sample of TMSS carbon stars. (*b*) Histogram of the $m(K_0)-m(12\ \mu\text{m})$ color for the sample of TMSS carbon stars.

FIG. 4.—(*a*) Distributions in $I-K$ for 22 R stars from the TMSS (*dashed histogram*) and 117 N stars from the TMSS (*solid histogram*). (*b*) As in (*a*), but for $K-m(12\ \mu\text{m})$ color. There is no evidence for color differences between the R- and N-type stars.

TABLE 3

STATISTICAL PROPERTIES OF CARBON STAR COLORS

	$(I-K)_0$	$[K-m(12\ \mu\text{m})]_0$
Mean.....	2.71	1.84
Standard deviation..	1.29	1.25
Maximum range	0.3–5.8	−0.6–9.4

temperatures of the coolest R-type stars and the warmest N-type stars.

Figure 5 shows a color-color diagram for the 193 stars in this sample which were detected at 60 μm in the *IRAS* survey. The departure from the colors expected for thermal emission is attributed to variations in the wavelength dependence of emissivity of grains in optically thin circumstellar envelopes. Analyses of the 12–100 μm colors of carbon stars have shown that, if the emission at these wavelengths is attributed to heated circumstellar dust having an emissivity that varies according to ν^{α}, then $\alpha \sim 1.1$ (Jura 1986; Zuckerman and Dyck 1986*b*).

The total luminosity of each star in our sample is listed in Table 4. The resultant range in luminosity, $\sim 6\times10^3$ to $\sim 4\times10^4\ L_{\odot}$, is in agreement with current models of stars on the asymptotic giant branch.

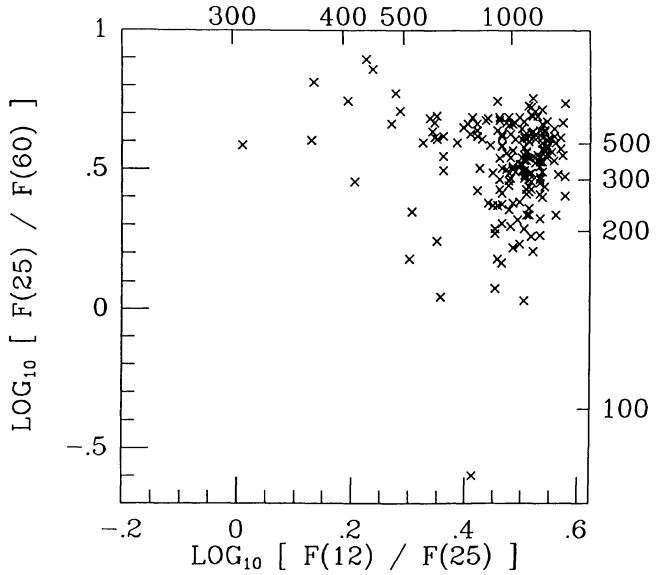

FIG. 5.—Color-color diagram for the TMSS sample of carbon stars. Equivalent color temperatures are plotted on the top and right-hand axis.

An average spectral energy distribution for stars in our sample is shown in Figure 6. To obtain this, we normalized the spectral energy distribution of each star by its total flux, and then computed the energy per octave (νF_{ν}) for each star at $\lambda = 0.9$, 2.2, 4.2, 12, 25, 60, and 100 μm. Figure 6 shows the average value of $\nu F_{\nu}/\int F_{\nu} d\nu$ at each of these wavelengths.

TABLE 4

DERIVED PROPERTIES OF CARBON STARS

TMSS	Distance (kpc)	Luminosity (10^4 $L_\odot$)	log dM/dt ($M_\odot$/yr.)	TMSS	Distance (kpc)	Luminosity (10^4 $L_\odot$)	log dM/dt ($M_\odot$/yr.)	TMSS	Distance (kpc)	Luminosity (10^4 $L_\odot$)	log dM/dt ($M_\odot$/yr.)
+40003	1.14	0.93	-7.02	+30110	1.05	0.84	-6.46	-10152	0.66	0.82	-6.98
+70003	1.31	0.94	-6.43	+30114	0.99:	1.01:	-6.17:	+10154	1.56	0.82	-6.63
+40006	0.62	0.75	-6.92	+10089	0.95	0.81	-6.84	+10156	1.57	0.79	-6.84
+40010	0.87	0.73	-6.60	-30046	1.43	0.87	-7.21	+10158	1.50	0.80	-6.85
+70009	1.31	0.88	-7.08	+20115	1.52	0.70	-6.75	+30182	1.51	1.30	-6.39
+60026	1.29	0.75	-6.87	+70064	1.44	0.87	-7.24	-20131	1.43:	1.03:	-5.86:
+60034	1.47	0.97	-6.53	-10095	1.43	0.94	-6.56	00158	1.52	0.80	-6.71
+50030	1.15	0.81	-6.34	+10094	1.00	0.93	-6.73	-30097	1.18	0.80	-6.53
+60041	0.87	0.93	-6.37	+20120	0.90	0.80	-6.82	-10177	1.52	0.76	-6.98
+30025	0.60	0.75	-7.03	+20121	0.49	0.78	-6.65	00162	1.51	0.97	-6.37
-30015	0.43	0.80	-6.12	+40140	1.49	1.03	-6.18	-30106	1.41	0.85	-6.66
+60056	1.25	0.78	-6.92	+30127	1.07	0.99	-6.97	-30114	1.20	0.76	-6.65
+60069	1.22	0.74	-6.87	+40141	1.44	0.86	-6.90	-20156	1.03	0.73	-6.80
+50061	1.34	0.88	-6.85	-10104	1.25	0.76	-7.45	00172	1.12	0.78	-6.74
-30021	0.77	1.07	-6.26	+40151	1.32	0.84	-6.40	-20165	1.45	0.70	-7.05
+60113	0.74	0.86	-6.99	+30143	0.65	1.18	-6.85	-30132	1.25	1.35	-6.31
+50088	1.20	0.88	-7.05	+10113	1.11	0.74	-6.82	-30133	1.47	0.75	-6.64
+50096	1.06:	1.97:	-5.31:	+10118	1.23	0.73	-6.41	-30134	0.94	0.97	-6.90
+60124	0.48	0.78	-6.53	00103	0.85	0.71	-6.93	+20206	0.45	0.76	-6.98
+50100	0.64	0.72	-6.66	+30150	1.53	0.85	-7.00	+20207	0.78	0.80	-6.79
+40067	1.15	0.81	-6.94	+10119	1.57	0.76	-6.79	-20184	1.28	0.94	-6.56
+40070	1.18:	0.96:	-5.81:	-30060	1.26	0.91	-6.69	+10216	0.29[a]	4.28	-4.45
+60138	1.07	0.96	-7.35	+10121	0.57	0.83	-7.00	-20199	0.54	0.55	
+30074	1.18	0.75	-6.94	-10122	1.38:	1.29:	-5.64:	+30219	0.71:	1.97:	-4.88:
+50115	0.95	0.83	-7.05	+20145	1.24	0.88	-6.70	-10236	1.40	1.97	
+40089	0.83	0.68	-6.65	+40157	1.54	0.92	-6.81	-30165	1.50	0.93	-6.24
+70055	0.50	0.81	-6.92	+20152	0.78	0.71	-6.78	-10242	0.31	0.79	-6.90
+20094	1.31	1.02	-7.01	+40158	0.30	0.75	-6.89	+70100	0.54	0.79	-6.95
+30098	0.64	0.80	-6.67	-10133	1.53	0.71	-7.08	-20218	0.34	0.69	-6.02
+40101	0.81	0.70	-6.91	+30163	1.34	0.87	-7.05	00217	0.59	0.80	-6.87
+50130	1.37	0.71	-6.73	00123	1.54	0.73	-7.19	+50219	0.29	0.77	-6.97
+20095	1.34	0.91	-6.98	-20101	1.31	0.94	-6.14	00224	1.02:	1.01:	-5.69:
-10080	0.43	0.87	-6.49	00125	1.44	0.86	-6.70	+70116	0.47	0.77	-6.87
+50135	0.82	0.73	-6.77	00127	1.57	0.83	-6.50	+40273	1.02	0.86	-6.36
00066	0.35	0.80	-6.89	00131	1.48	1.05	-6.28	-10339	0.83	0.77	-6.95
+40115	1.11	0.91	-6.91	00136	1.22	0.86	-6.96	-30268	0.68	0.74	-6.90
-10083	1.24	0.87	-6.86	+10144	0.94	0.84	-6.36	-30277	1.39	0.94	-6.74
+10081	0.94	0.80	-6.65	+10146	1.00	0.91	-6.88	-30293	0.92	0.74	-6.91[b]
+40120	1.29	0.98	-7.16	00141	1.04	0.85	-6.82	-20364	0.46	0.70	-6.97
+10083	1.09	0.77	-6.69	-10149	0.69	0.78	-6.77	-20382	1.01	0.80	-6.74

TABLE 4—*Continued*

TMSS	Distance (kpc)	Luminosity (10^4 $L_\odot$)	log dM/dt ($M_\odot$/yr.)	TMSS	Distance (kpc)	Luminosity (10^4 $L_\odot$)	log dM/dt ($M_\odot$/yr.)	TMSS	Distance (kpc)	Luminosity (10^4 $L_\odot$)	log dM/dt ($M_\odot$/yr.)
-30333	1.04	0.64	-6.95[b]	+30374	1.45:	2.35:	-5.15:	+50409	0.86	0.86	-7.00
+60255	0.69	0.83	-6.28	+30382	0.97	0.87	-6.57	+20523	1.17	0.53	
-20420	1.34	0.81	-6.33[b]	+30385	1.48	0.88	-6.38	+30484	1.47	0.74	-6.59
-10396	1.18:	1.16:	-5.45:	+20435	1.36	0.73	-7.00	+50418	1.17	0.78	-6.54
-10397	1.45	0.93	-6.95[b]	+30392	1.42	0.75	-6.92[b]	+60358	1.29	0.70	-7.02[b]
-30364	1.18	1.31	-6.48	+40368	0.74	0.73	-6.91	+60365	0.88	0.89	-6.80
-30365	1.18	0.81	-6.19	+30408	1.48	0.86	-7.03[b]	+50455	1.40	0.95	-6.95
-10409	0.85	0.77	-6.84[b]	+20452	0.97	0.77	-6.76	+60393	0.95	0.78	-6.03
-20464	1.38	0.90	-7.21[b]	+50316	0.95	0.76	-6.88	+60403	1.33	0.89	-6.86
-20482	1.16	1.49	-5.83	+40389	1.46	0.70	-6.81[b]	+60409	1.28:	2.08:	-5.44:
00351	1.07	0.70	-6.70	+30416	1.56	0.82	-6.46	+60411	0.96:	0.91:	-5.96:
-20488	1.24	0.95	-6.72	+40391	1.24	0.86	-7.25[b]	+60412	1.33	0.93	-5.75
00353	0.90	0.73	-6.83	+40393	1.14	0.80	<-7.08[b]	+40540	1.18	2.39	-4.87
-10433	0.63	1.11	-7.29	+40397	0.67	0.79	-6.99	00532	0.28	0.77	-7.14
+40321	0.51	0.73	-6.94	-20585	0.52	0.74	-7.02	+60433	0.48	0.70	-7.17
-10441	1.03	0.48		+40403	1.09	0.68	-7.14[b]				
+20370	1.00:	2.85:	-5.32:	+50324	0.84	0.81	-6.39				
00365	1.28:	2.85:	-5.17:	+40417	1.12	0.71	-7.32[b]				
+40325	0.90	0.75	-6.87	+40436	1.14	0.72	-6.66[b]				
-20518	1.35	0.82	-6.88	+50338	0.58:	1.42:	-5.73:				
+10379	0.99	0.72	-6.32	+30447	1.48	0.85	-6.66				
-10467	0.52	0.79	-6.67	+30456	1.25	0.84	-6.45				
-10469	1.36	0.85	-6.40	+50346	1.44	0.43					
-10475	1.31	0.99	-7.17	00499	0.81:	1.08:	-5.72:				
00402	0.84	0.70	-5.93	+50357	1.64:	1.40:	-5.18:				
+10389	0.87	0.78	-6.83	+40478	1.30	0.89	-6.93				
00404	1.36	0.80	-6.55	+70170	1.18	0.92	-6.29				
+10397	1.05	0.76	-6.85	+40484	1.31	0.75	-6.73				
+10401	1.37:	2.32:	-5.22:	+40485	1.03:	1.17:	-5.55:				
-10486	0.38	0.77	-6.89	+60321	1.41	0.94	-6.71				
00418	1.45	1.16	-7.55[b]	+80048	0.39	0.81	-6.50				
+20393	0.88	0.74	-6.81	+70172	1.44	0.86	-6.90				
-20554	1.32	1.35	-6.38	+50388	1.61	1.19	-6.13				
-10502	0.92:	1.49:	-5.35:	+50389	0.99	0.76	-6.87				
+40345	1.12	0.82	-6.78	+40489	0.48	0.77	-6.79				
+80036	0.44	0.73	-7.13	+40491	0.48	0.74	-6.66				
+20406	1.42	0.77	-6.93	+70177	0.67	0.79	-7.49				
+50295	1.00	0.78	-6.74	+50399	1.44	0.73	-6.77				
00438	1.31	1.00	-6.25	+50403	1.37	0.82	-6.77				
-20568	0.56	0.75	-6.84	+50408	1.02	0.82	-6.71				

NOTE.—A colon is listed next to each entry if $F_{12\ \mu m} > F_{2\ \mu m}$, which suggests that the distances are overestimated (see text).

[a] We have adopted a distance for TMSS +10216 of 290 pc (see text). The luminosity and mass-loss rate are estimated on the basis of this value of the distance.

[b] These mass-loss rates are based on the flux at 25 μm, since the *IRAS* satellite did not detect them at 60 μm (see text).

The error bars shown in Figure 6 are formal standard errors from the mean of all the stars. As expected, the total luminosities of the carbon stars in our sample are dominated by emission from 0.9 to 5 μm, even for the reddest object, TMSS +10216.

The relationships between period and $(I-K)_0$ and $m(K_0)-m(12\ \mu\text{m})$ colors for the 96 stars in our sample with known periods is shown in Figure 7. The best (least-squares) linear fits to these data are

$$P(\text{days}) = (61\pm4)(I-K)_0+102\pm1.3, \qquad r=0.6,$$

$$P(\text{days}) = (219\pm2)[K_0 - m(12\ \mu\text{m})] - 64\pm0.8, \quad r=0.6,$$

where r is the normalized correlation coefficient of the fit. Thus marginally significant positive correlation exists between period and color for these stars. In any case, stars with periods exceeding 400 days have significantly redder mean colors than stars with shorter periods. This conclusion is similar to that obtained by Jura (1986), who studied carbon stars selected from the GCVS (a sample which overlaps with the present one), and by DeGioia-Eastwood *et al.* (1981) for oxygen-rich stars. The implications of these results are discussed further in § VII.

We find no correlation between period and bolometric luminosity, as illustrated in Figure 8. This is, perhaps, not surprising, since (1) the majority of stars in our sample have a narrow range in bolometric correction and (2) we have assumed that all stars in our sample have the same value of $M(K)$. On the basis of observations of the LMC, Glass *et al.* (1987) report a period–apparent K-magnitude relationship for long-period variables, including carbon stars. For a dis-

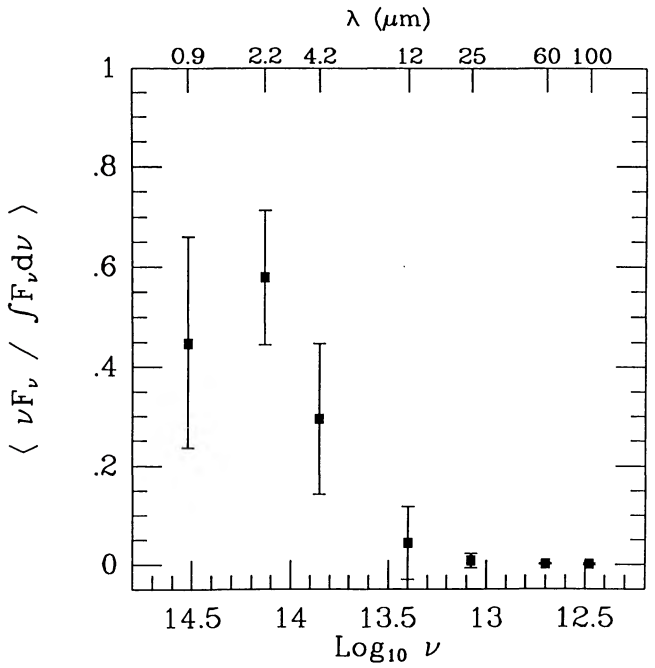

FIG. 6.—Average spectral energy distribution for the TMSS sample of carbon stars, plotted as the flux per octave at each of the observed wavelengths normalized to the total flux. Note that the total flux is derived by adding *all* the energy, including that from the wavelengths in between the observed bands. The vertical error bars represent 1 formal standard deviation from the mean of all the stars in the TMSS sample.

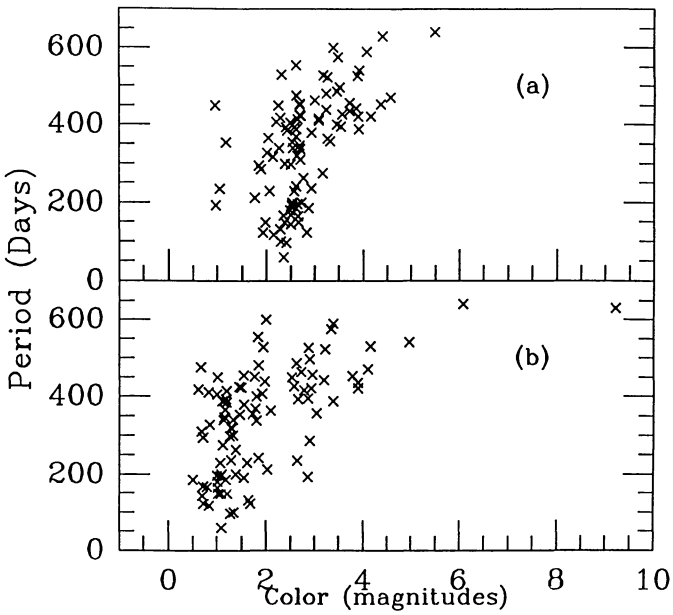

FIG. 7.—(*a*) Distribution of the known periods of 96 sources from the TMSS sample with $(I-K)_0$ color. (*b*) As in (*a*), but with $m(K_0)-m(12\ \mu\text{m})$ color. Stars with periods longer than about 400 days tend to have redder mean colors than those stars with shorter periods.

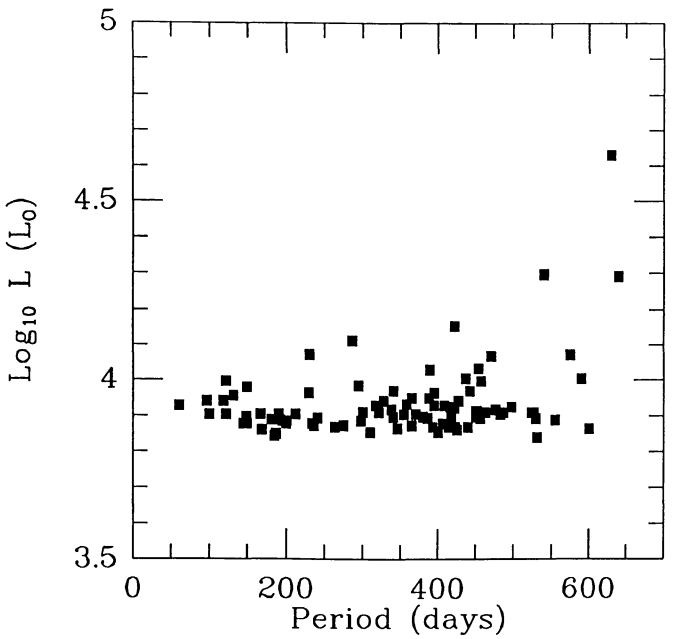

FIG. 8.—Distribution of known periods as a function of derived bolometric luminosity.

tance modulus to the LMC of 18.5 mag, their result gives

$$M(K) = 1.0 - 3.5 \log P,$$

where P is the period in days. According to this relationship, we would expect that $M(K)$ would vary by more than a magnitude between stars with $P \leq 200$ days and those with $P \geq 400$ days. Such a difference in the absolute magnitude should mean that in our magnitude-limited sample we have overestimated the mean distance to the shorter period stars or underestimated the distances to the longer period stars. If we assume that the two populations have intrinsically the same scale height, this would mean that our inferred scale height for the shorter period stars would be significantly larger than the inferred scale height for the longer period stars. In fact, there is no significant difference in the mean height above the Galactic plane for the 19 stars with $P \leq 200$ days ($|z| = 180$ pc) and the 31 stars with $P \geq 400$ days ($|z| = 190$ pc). Therefore, we find no evidence for a similar period-luminosity relationship for carbon stars in the local Milky Way.

VI. SPACE DISTRIBUTION

Given the assumption of constant absolute K-magnitude for all of the carbon stars in our sample [$M(K) = -8.1$] and the limit of the TMSS (+3.0 mag), the present sample should include all carbon stars within 1.5 kpc of the Sun. Comparisons with other surveys of carbon stars show the extent to which this expectation is fulfilled. At $b > +30°$, the Case survey finds 44 R-type carbon stars and 14 N-type carbon stars, whereas the TMSS finds only one R-type star but eight N-type carbon stars. Thus the TMSS is relatively less sensitive to R-type than to N-type carbon stars. If the Case survey had sufficient sensitivity to detect most of the R- and N-type carbon stars at these latitudes, then the R-type stars must be significantly less luminous at 2.2 μm than the N-type stars. Neglecting the uncertainty that results from the overlap between the R- and N-type classifications, and assuming that both groups of stars have the same scale height (which is much less than the distance to which they could be seen in the Case survey), we estimate that the R-type stars may have K-band luminosities that are an order of magnitude lower than N-type stars. Since we have assumed that all carbon stars in the TMSS have the same absolute K-magnitude, the distances to R-type stars in our sample may be overestimated; available data suggest, however, that fewer than 15% of the carbon stars in the TMSS may be classified as type R.

Comparison of the TMSS with the RAFGL survey (§ II) showed that the TMSS missed 37 extremely red [$m(K) - m(12\ \mu\text{m}) > 4$ mag] stars that fell in the region of sky it covered. Kinematic distances for 20 of these stars can be estimated from radial velocities obtained from observations of their CO line emission (Knapp and Morris 1985; Zuckerman and Dyck 1986*a*; Zuckerman, Dyck, and Claussen 1986). Concentrating on those lying within 10° of the Galactic plane (15 out of the 20), we find that 6 (or 40%) have distances less than 1.5 kpc. We thus estimate that ~15 of the carbon stars detected in the RAFGL survey but missed in the TMSS lie within the volume sampled by the TMSS, so that the TMSS gives a 7% underestimate of the number of carbon stars within this distance of the Sun. Presumably, the faintness of these missing stars at 2.2 μm may be attributable to extinction of starlight by dust in massive circumstellar envelopes. Only 12 stars in the present sample have $K - m(12\ \mu\text{m})$ colors as red as the carbon stars found only in the RAFGL survey, i.e., > 4 mag. TMSS +10216 is the most notable of these. The foregoing argument suggests that the distances to these stars may be overestimated by assuming that their K-band luminosity matches that of other carbon stars in our sample. In particular, the estimate of the distance to TMSS +10216 by this method is 790 pc; we have adopted a distance of 290 pc (Herbig and Zappala 1970) for this source. Recent studies (Zuckerman, Dyck, and Claussen 1986) suggest that the distance to this source may be even smaller than this.

The distances to all carbon stars in the TMSS sample, derived by assuming that all have $M(K) = -8.1$ mag, are presented in Table 4. For those stars with $K - m(12\ \mu\text{m}) > 3.4$ ($F_{12\ \mu\text{m}} > F_K$), the distance is probably overestimated, and we have indicated that uncertainty by marking the values with a colon. The values of the distances are ~20% larger than those derived by Knapp and Morris (1985). They should also be ~20% larger than those derived by Fuenmayor (1981), since he assumed $M(I) = -5$ for the carbon stars in his sample, and since the stars in the TMSS sample have a mean $(I - K)_0$ of 2.7. Our distances are also 2.2 times the distances derived by Bergeat, Lunel, and Sibille (1978) from a model of the circumstellar envelopes of carbon stars and available kinematic data. On the other hand, the distances we compute are typically 4 times smaller than those estimated by Thronson *et al.* (1987), since their estimate of the mean 12 μm luminosity is about 15 times higher than that derived here on the basis of the assumed absolute K-magnitude for carbon stars and their mean $K - m(12\ \mu\text{m})$ color.

Using distances given in Table 4, and correcting for the regions of the sky not covered by the TMSS, we find that the distribution of TMSS carbon stars with height above the Galactic plane can be described by an exponential,

$$N(z) = N_0 \exp\left(-\frac{z}{z_0 \times 10^{-0.4[M(K)+8.1]}}\right),$$

where N_0 is the volume number density in the Galactic plane, 2.3 ± 0.1 dex, and z_0 is the scale height, 2.0 ± 0.4 dex; the errors in these values are dominated by the dispersion in the absolute K-magnitudes of carbon stars (0.6 mag) and the uncertainty of the distance to the Magellanic Clouds (0.2 mag). Figure 9*a* shows this distribution with Galactic latitude, and the fit as described above for $z_0 = 150$, 200, and 250 pc. The deduced scale height is marginally smaller than that determined for the carbon stars with $J = 1 \rightarrow 0$ rotational CO line emission studied by Knapp (1983) (2.4 dex) and for OH maser stars in the solar neighborhood (2.45 dex). It more closely approximates the scale height (2.3 dex) of OH maser

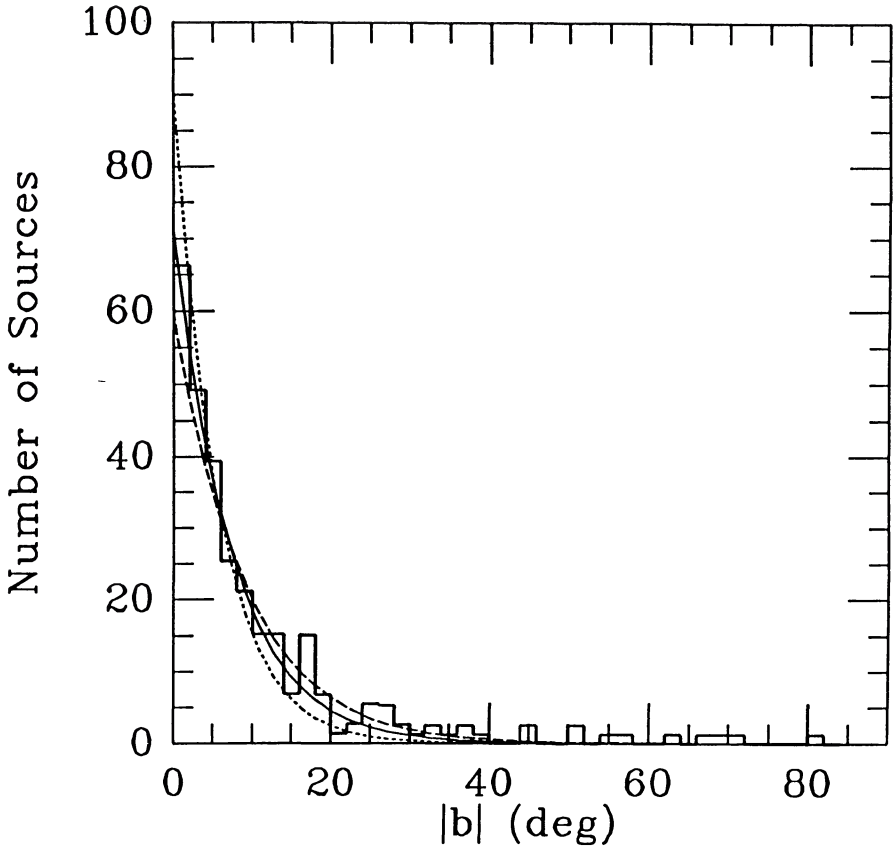

FIG. 9*a*

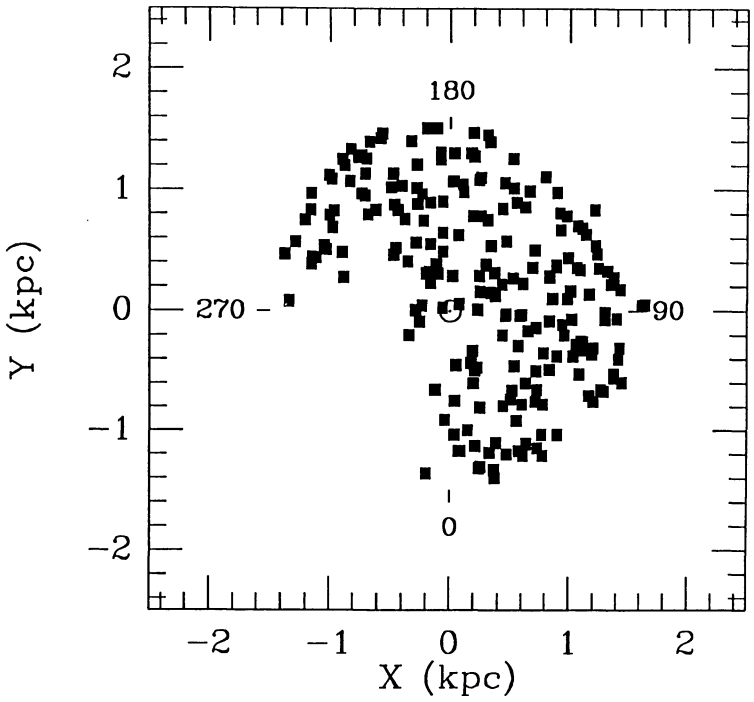

FIG. 9*b*

FIG. 9.—(*a*) Histogram of the number of carbon stars vs. absolute Galactic latitude, corrected for the incomplete sky coverage of the TMSS. The best least-squares fit to an exponential distribution in z is given by the solid curve; the derived scale height is 200 pc. Dotted and dashed curves are distributions with scale heights of 150 and 250 pc, respectively, normalized by the area of the fitted curve. (*b*) Distribution of carbon stars projected onto the Galactic plane. The cardinal longitude points are labeled. The apparent lack of sources in the longitude range 270°–0° is due to the incomplete sky coverage of the TMSS: the southern declination limit is −33°. The distribution appears to be fairly uniform in the region of the sky observed.

stars with large (20–30 km s^{-1}) outflow velocities (Herman and Habing 1985). Recent models of the Galaxy (e.g., Mihalas and Binney 1981) suggest that stars having the scale height estimated here for the TMSS carbon stars belong to an intermediate-to-old disk population.

To estimate the mass of carbon star progenitors, we use the tabulation of Miller and Scalo (1979) for the scale heights of main-sequence stars as a function of spectral class. They show that stars with a mean scale height of 200 pc have a mass between 1.2 and 1.4 $M_\odot$, a value fully consistent with previous estimates of the masses of progenitors of carbon stars (see, for example, Dean 1976; Dominy 1984). Because the scale heights of stars increase with time, there may be some objects in our sample with progenitor masses exceeding 1.4 $M_\odot$. In any case, few of the carbon stars in this sample have main-sequence masses exceeding 1.6 $M_\odot$, or less than 1.2 $M_\odot$. Although the metallicity in the Magellanic Clouds is different from that in the Milky Way, and the mechanism of carbon star formation is sensitive to metallicity (see Iben and Renzini 1983), it is notable that Aaronson and Mould (1985) find carbon stars only in clusters older than $\sim 0.8\times10^9$ yr, which implies that the masses of the main-sequence progenitors are ≤ 2.5 $M_\odot$. Zuckerman, Dyck, and Claussen (1986) have recently found that carbon stars with large CO line widths typically have smaller average Galactic latitudes than those with narrower line widths, implying that they may represent a different population.

The projected radial distribution of the carbon stars in our sample is shown in Figure 9*b*. It appears uniform over the region observed to a distance of 1.5 kpc. Like Blanco (1965), we find no concentration of carbon stars toward the Galactic center. We also fail to detect an asymmetry with Galactic longitude at the level deduced by Fuenmayor (1981). In fact, the TMSS finds the same surface density of carbon stars in each of the two regions of Fuenmayor's survey (one centered at the Galactic center, and one centered at the anticenter), i.e., 0.037 ± 0.011 stars per square degree.

We estimate the disk surface density of carbon stars in the solar neighborhood to be 1.6 ± 0.2 dex. Correcting for the carbon stars that lie within 1.5 kpc of the Sun but were missed by the TMSS because of their redness, we derive a density of 43 carbon stars per square kiloparsec. If this surface density is uniform, then the total number of carbon stars within a galactocentric radius $R=15$ kpc is $\sim 3\times10^4$.

VII. THE MASS-LOSS RATE AND THE MASS RETURNED TO THE INTERSTELLAR MEDIUM

An expression for the time-averaged mass-loss rate from a circumstellar envelope has been developed by Jura (1987) assuming a constant dust-to-gas ratio, and assuming a dust grain emissivity at 60 μm of 150 cm^2 g^{-1}. It is

$$\frac{dM}{dt} = 1.7\times10^{-7} v_{15} r_{\rm kpc}^2 F_{\nu,60} \left(\frac{\lambda_{10}}{L_4}\right)^{1/2},$$

where v_{15} is the outflow velocity in units of 15 km s^{-1}, $r_{\rm kpc}$ is the distance to the star in kiloparsecs, L_4 is the luminosity in units of 10^4 $L_\odot$, $F_{\nu,60}$ is the flux at 60 μm in janskys, and λ_{10} is the mean wavelength of the light emerging from the star and its circumstellar shell in units of 10 μm.

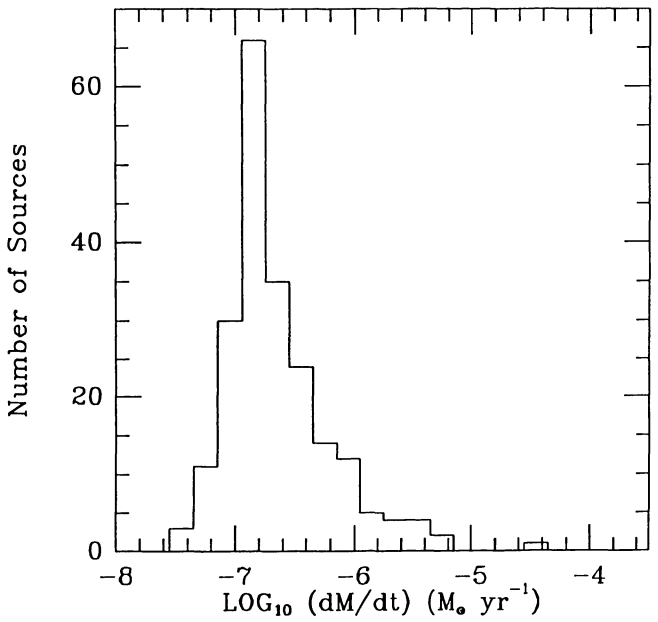

FIG. 10.—Histogram of the logarithm of the mass-loss rates for the TMSS carbon stars detected at 60 μm with *IRAS*. The large peak occurs at about 2.0×10^{-7} $M_\odot$ yr^{-1}

We have assumed, for our sample, that $v_{15}=1$, and that $\lambda_{10}=0.22$ (see Fig. 4), except for those stars with $m(K)-m(12\ \mu{\rm m})\geq 3.5$ mag, in which case we adopt $\lambda_{10}=1.0$. For those stars with only upper limits to the 60 μm flux, we have estimated the mass-loss rate using the 25 μm flux, with the numerical coefficient in the above relation replaced by 4.0×10^{-8}, since a typical value for the ratio of the flux at 25 μm to that at 60 μm is 4.5 (Zuckerman and Dyck 1986*b*). One star (TMSS +40393) was not detected in either of the 25 or 60 μm bands, and an upper limit to the mass-loss rate is shown for that star. The results are listed in Table 4 and shown as a histogram in Figure 10. The peak of the distribution is 2.0×10^{-7} $M_\odot$ yr^{-1}, and the half-peak values are 7.9×10^{-8} and 3.2×10^{-7} $M_\odot$ yr^{-1}. The total range of the distribution is about 3 orders of magnitude, from 3.2×10^{-8} to 4.3×10^{-5} $M_\odot$ yr^{-1}. With the exception of TMSS −30015, which has very unusual colors, the mass-loss rates in Table 3 usually agree to within a factor of 2 with those estimated by Knapp and Morris (1985) for the 14 stars common to both studies, when they are corrected to the same distance. Our mass-loss rates also agree within a factor of 2 with the estimates provided by Olofsson, Eriksson, and Gustafsson (1987). These comparisons reflect the constancy of the dust-to-gas ratio in carbon stars.

Figure 11 illustrates the relationship between period and mass-loss rate for carbon stars with large amplitudes at 2.2 μm (>0.5 mag) and those with smaller amplitudes. A strong correlation between period and mass-loss rate is not observed; however, the highest mass-loss rates occur only among carbon stars with periods above ~ 300 days, and among those carbon

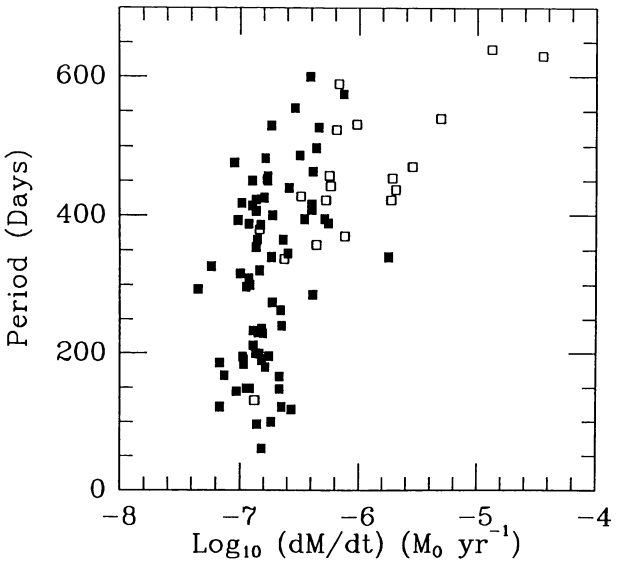

FIG. 11.—Period vs. the mass-loss rate. Open squares represent those carbon stars with periods which have K amplitudes (2.2 μm) greater than 0.5 mag as determined from the TMSS or a comparison of the TMSS with the data from Noguchi *et al.* (1981). Filled squares represent those carbon stars with periods which have K amplitudes less than 0.5 mag.

stars with higher near-infrared amplitudes. These results imply that the phase of high mass-loss rates among carbon stars occurs during periods of Mira-like variability.

Compared with the distribution function of mass-loss rates deduced by Knapp and Morris (1985), which is nearly independent of mass-loss rate, the distribution of mass-loss rates of the TMSS sample shows a strong peak at a value near the minimum of the range of their estimates. This is not unexpected, since, as Knapp (1987) points out, the CO-selected sample of Knapp and Morris is strongly biased toward stars with high mass-loss rates. Recently, Knapp and Wilcots (1987) studied a sample of *IRAS* sources within 30° of the Galactic poles, and deduced that many more stars in this sample have low mass-loss rates than in the CO-selected sample. Also, the CO study of bright N stars by Olofsson, Eriksson, and Gustafsson (1987) shows that mass-loss rates of about 10^{-7} $M_\odot$ yr^{-1} are common among those stars.

The integrated rate of mass return to the Galaxy from carbon stars is estimated on the assumption that their local space density is uniform over galactocentric radii $0 < R(\mathrm{kpc}) < 15$. Using the distribution of mass-loss rates for carbon stars in the TMSS, we find $(dM/dt)_{\mathrm{tot}} = 0.013 \times (R/15)^2$ $M_\odot$ yr^{-1}, corrected for the incomplete sky coverage of the TMSS. This value is dominated by only a few stars; the mass-loss rate for TMSS +10216 accounts for nearly a third of the total mass-return rate from our sample.

The total mass return from carbon stars determined from the TMSS sample is about an order of magnitude smaller than suggested by Knapp and Morris (1985), who estimate equal contributions from both carbon stars and M stars with a total greater than 0.3 $M_\odot$ yr^{-1}. However, according to the discussion in § VI, the TMSS undersamples extremely red stars like TMSS +10216. To estimate their mass-loss rates, we note that recent time-series observations of stars found in the RAFGL but not in the TMSS show that these stars typically have infrared (K-band) amplitudes as great as or greater than that of TMSS +10216. Given our previous estimate, that 15 stars of this type are located within 1.5 kpc of the Sun but are missing from the TMSS sample, and assuming that each of these has a mass-loss rate equivalent to that of TMSS +10216, then the total mass return from carbon stars may be ~5 times higher than that estimated from the TMSS stars alone. This value is in good agreement with that derived previously by Knapp and Morris (1985) from a CO-selected sample.

VIII. THE CARBON STAR PHASE IN STELLAR EVOLUTION

In the previous section we showed that most of the carbon stars near the Sun are losing mass at a rate $\geq 2 \times 10^{-7}$ $M_\odot$ yr^{-1}. Because these stars have main-sequence masses mainly between 1 and 1.5 $M_\odot$, it is difficult to imagine that they can persist in the carbon star phase for much longer than 10^6 yr; otherwise they would lose too much material. This inferred lifetime of 10^6 yr is consistent with the analysis of LMC carbon stars by Richer (1981) and with theoretical predictions for the duration of the mass-losing phase of asymptotic giant branch evolution (Becker and Iben 1980; Bertelli *et al.* 1986; Iben and Renzini 1983), which seems the appropriate stellar evolutionary phase to assign to carbon stars. From our derived surface density of 43 stars kpc^{-2} and an upper limit to the lifetime of 10^6 yr, we find that the birthrate of carbon stars in the solar neighborhood is $\geq 4.3 \times 10^{-11}$ pc^{-2} yr^{-1}.

Miller and Scalo (1979) have compiled a large amount of empirical data and theoretical models to synthesize the stellar population in the neighborhood of the Sun. From their Tables 1 and 2, the birthrate of stars with masses between 1.2 and 2 $M_\odot$ in the solar neighborhood is 4×10^{-10} stars pc^{-2} yr^{-1}. Therefore, at least ~10% of all main-sequence stars between 1.2 and 2 $M_\odot$ eventually pass through a carbon star phase. In fact, if the duration of the carbon star phase is appreciably less than 10^6 yr, an even larger fraction of all these main-sequence objects must become carbon stars. A lower limit to the duration of the carbon star phase is 10^5 yr if *all* main-sequence F stars eventually become carbon stars. Even if the main-sequence progenitors of carbon stars have masses which range up to 6 $M_\odot$, the lifetime of the carbon star phase can be no less than 5×10^4 yr, since the birthrate of stars in the mass range 1.2–6 $M_\odot$ is only 8×10^{-10} stars pc^{-2} yr^{-1} (Miller and Scalo 1979). On the basis of the detection of oxygen-rich features in the spectra of carbon-rich stars, Willems and de Jong (1986) estimate the duration of the carbon star phase to be between 10^3 and 10^4 yr. Their results can be reconciled with ours only by making the unsupported hypothesis that stars oscillate quite frequently between being oxygen-rich and carbon-rich as they evolve on the asymptotic giant branch. Alternative models for the existence of silicate emission features around carbon-rich stars also exist (Little-Marenin and Benson 1987) which do not require such a short duration of the carbon star phase of evolution. Finally, it seems that since carbon stars are currently on the asymptotic giant branch, they eventually will evolve into planetary nebulae (Zuckerman

et al. 1978). Our conclusion that at least 10% of all $\sim 1.5\ M_\odot$ stars become carbon stars is fully consistent with the result reported by Zuckerman and Aller (1986) that approximately half of all planetary nebulae are carbon-rich.

IX. CONCLUSIONS

The similarity in colors and spectral type of carbon stars found in the TMSS and in the Magellanic Clouds suggests that they share the same narrow range in absolute K-magnitude. To the extent that all carbon stars have the same absolute K-magnitude, the TMSS provides a volume-limited sample of carbon stars within 1.5 kpc of the Sun. Comparisons of the TMSS sample of carbon stars with other surveys shows the expected result that surveys carried out at shorter wavelengths miss some of the reddest stars found in the TMSS, and that the TMSS fails to detect some of the reddest carbon stars found in mid-infrared surveys. A minority of carbon stars must therefore have lower K-band luminosities than the value assumed here.

Infrared colors of carbon stars in the TMSS are generally nonphotospheric; strong excesses are apparent at mid- and far-infrared wavelengths. These excesses are attributed to emission from dust in circumstellar envelopes associated with the stars. Carbon stars are commonly optical variables, but only a few of those sampled by the TMSS show large ($\Delta K \geq 0.5$ mag) variations at 2.2 μm.

The scale height perpendicular to the Galactic plane for carbon stars is 200 pc. This value suggests that the main-sequence progenitors of most carbon stars are probably F-type stars, since stars of this mass have a similar scale height (Miller and Scalo 1979).

The surface density of carbon stars in the Galaxy is roughly uniform within the volume sampled ($r < 1.5$ kpc). Including extremely red stars detected at mid-infrared wavelengths, it is 43 kpc^{-2}. In contrast with the results of Fuenmayor (1981), no evidence of any asymmetry in the distribution of carbon stars with Galactic longitude is apparent. This difference may be attributed to the reduction of interstellar extinction at 2.2 μm compared with surveys at shorter wavelength.

The rate of mass return to the Galaxy from this flux-limited sample of carbon stars is found to be significantly less than estimated previously from samples selected at wavelengths dominated by emission from their circumstellar envelopes. Most of the mass lost by carbon stars comes from a few of the reddest objects, typically those with high infrared amplitudes of variability. We deduce that the mass-loss mechanism among these stars must be related to their pulsations. The mass-loss rate of extremely red objects like TMSS +10216 is nearly half that of all other carbon stars in the TMSS combined. The red carbon stars that were missed in the TMSS because of the heavy obscuration of their circumstellar envelopes have infrared amplitudes similar to that of TMSS +10216 and may eject more than an order of magnitude more mass per unit volume per unit time than all of the carbon stars found in the TMSS.

This paper relied heavily on an unpublished compilation of spectral classification and identifications of sources in the TMSS by C. Payne-Gaposchkin. We would like to thank D. McGonagle for his help in producing the tables, and W. Buscombe for pointing out some variable star names. We also wish to thank F. C. Gillett, B. Madore, P. Schechter, R. Jedrzejewski, and B. Zuckerman for helpful comments on the manuscript. This work was partially supported by the AFOSR, under grant 85-0057, and by the National Aeronautics and Space Administration under JPL contract 947690. M. J. acknowledges support from NASA and the National Science Foundation.

REFERENCES

Aaronson, M., and Mould, J. 1985, *Ap. J.*, **288**, 551.
Baumert, J. H. 1974, *A.J.*, **79**, 1287.
Becker, S. A., and Iben, I. 1980, *Ap. J.*, **237**, 111.
Becklin, E. E., Frogel, J. A., Hyland, A. R., Kristian, J., and Neugebauer, G. 1969, *Ap. J. (Letters)*, **158**, L133.
Bergeat, J., and Lunel, M. 1980, *Astr. Ap.*, **87**, 139.
Bergeat, J., Lunel, M., and Sibille, F. 1978, *Astr. Ap.*, **64**, 423.
Bertelli, G., Bressan, A. G., Chiosi, C., and Angerer, K. 1986, *Astr. Ap. Suppl.*, **66**, 191.
Bidelman, W. P. 1980, *Pub. Warner and Swasey Obs.*, Vol. **2**, No. 6.
Blanco, V. M. 1965, in *Stars and Stellar Systems*, Vol. **5**, *Galactic Structure*, ed. W. A. Blaauw and M. Schmidt (Chicago: University of Chicago Press), p. 241.
Blanco, V. M., McCarthy, M. F., and Blanco, B. M. 1980, *Ap. J.*, **242**, 242.
Blanco, V. M., and Nassau, J. J. 1957, *Ap. J.*, **125**, 408.
Cannon, A. J., and Pickering, E. C. 1918–1924, *The Henry Draper Catalogue* (*Ann. Astr. Obs. Harvard College*, Vols. **91–99**).
Cohen, J. G., Frogel, J. A., Persson, S. E., and Elias, J. E. 1981, *Ap. J.*, **249**, 481.
Dean, C. A. 1976, *A.J.*, **81**, 364.
DeGioia-Eastwood, K., Hackwell, J. A., Grasdalen, G. L., and Gehrz, R. D. 1981, *Ap. J. (Letters)*, **245**, L75.
Dominy, J. F. 1984, *Ap. J. Suppl.*, **55**, 27.
Dyck, H. M., Lockwood, G. W., and Capps, R. W. 1974, *Ap. J.*, **189**, 89.
Frogel, J. A., Persson, S. E., and Cohen, J. G. 1980, *Ap. J.*, **239**, 495.
Frogel, J. A., and Richer, H. B. 1983, *Ap. J.*, **275**, 84.
Fuenmayor, F. J. 1981, *Rev. Mexicana Astr. Ap.*, **6**, 83.
Glass, I. S., Catchpole, R. M., Feast, M. W., Whitelock, P. A., and Reid, I. N. 1987, in *Late Stages of Stellar Evolution*, ed. S. Kwok and S. R. Pottasch (Dordrecht: Reidel), p. 51.
Hacking, P., *et al.* 1985, *Pub. A.S.P.*, **97**, 616.
Hansen, O. L., and Blanco, V. M. 1973, *A.J.*, **78**, 669.
_____. 1975, *A.J.*, **80**, 1011.
Herbig, G. H., and Zappala, R. R. 1970, *Ap. J. (Letters)*, **162**, L15.
Herman, J., and Habing, H. 1985, *Phys. Rept.*, **124**, 255.
Hoffleit, D., and Jaschek, C. 1982, *The Bright Star Catalogue* (4th rev. ed.; New Haven: Yale University Observatory).
Iben, I., and Renzini, A. 1983, *Ann. Rev. Astr. Ap.*, **21**, 271.
IRAS Catalogs and Atlases, Explanatory Supplement. 1985, ed. C. A. Beichman, G. Neugebauer, H. J. Habing, P. E. Clegg, and T. J. Chester (Washington, DC: GPO).
IRAS Point Source Catalog. 1985, Joint *IRAS* Science Working Group (Washington, DC: GPO) (PSC).
Jaschek, C. 1985, in *Cool Stars with Excesses of Heavy Elements*, ed. M. Jaschek and P. C. Keenan (Dordrecht: Reidel), p. 3.
Johnson, H. L. 1965, *Ap. J.*, **141**, 123.
Jura, M. 1986, *Ap. J.*, **303**, 327.
_____. 1987, *Ap. J.*, **313**, 743.
Keenan, P. C., and Morgan, W. W. 1941, *Ap. J.*, **94**, 501.
Kleinmann, S. G., Gillett, F. C., and Joyce, R. R. 1981, *Ann. Rev. Astr. Ap.*, **19**, 411.
Knapp, G. R. 1983, in *IAU Colloquium 76, The Nearby Stars and the Stellar Luminosity Function*, ed. A. G. Davis Philip and A. R. Upgren (Schenectady: Davis), p. 113.
_____. 1985, *Ap. J.*, **293**, 273.
_____. 1987, in *Late Stages of Stellar Evolution*, ed. S. Kwok and S. R. Pottasch (Dordrecht: Reidel), p. 103.
Knapp, G. R., and Morris, M. 1985, *Ap. J.*, **292**, 640.
Knapp, G. R., Phillips, T. G., Leighton, R. B., Lo, K.-Y., Wannier, P. G., Wootten, H. A., and Huggins, P. J. 1982, *Ap. J.*, **252**, 616.
Knapp, G. R., and Wilcots, E. M. 1987, in *Late Stages of Stellar Evolution*, ed. S. Kwok and S. R. Pottasch (Dordrecht: Reidel), p. 171.
Koester, D., Schulz, H., and Weidemann, V. 1980, *Astr. Ap.*, **81**, 145.

Kukarkin, B. V., *et al.* 1969–1971, *General Catalogue of Variable Stars*, Vols. **1–3** (3d ed.; Moscow: Sternberg State Astronomical Institute, Moscow State University) (GCVS).
Lee, O. J., Baldwin, R. B., Hamlin, D. W., Bartlett, T. J., and Gore, G. D. 1947, *Ann. Dearborn Obs.*, Vol. **5**.
Little-Marenin, I., and Benson, P. 1987, *Ap. J.*, in press.
Lockwood, G. W. 1974, *Ap. J.*, **192**, 113.
Lockwood, G. W., and McMillan, R. S. 1971, *Kitt Peak Obs. Contr.*, No. 554.
Lockwood, G. W., and Zinter, T. A. 1973, *A.J.*, **78**, 471.
Lucke, P. B. 1978, *Astr. Ap.*, **64**, 367.
Mazzitelli, I., and D'Antona, F. 1986, *Ap. J.*, **311**, 762.
Merrill, K. M., and Stein, W. A. 1976, *Pub. A.S.P.*, **88**, 294.
Mihalas, D., and Binney, J. 1981, *Galactic Astronomy*: *Structure and Kinematics* (San Francisco: Freeman).
Miller, G. E., and Scalo, J. M. 1979, *Ap. J. Suppl.*, **41**, 513.
Nassau, J. J., and Blanco, V. M. 1954*a*, *Ap. J.*, **120**, 118.
_____. 1954*b*, *Ap. J.*, **120**, 129.
_____. 1957, *Ap. J.*, **125**, 195.
_____. 1958, *Ap. J.*, **128**, 146.
Nassau, J. J., Blanco, V. M., and Cameron, D. M. 1956, *Ap. J.*, **124**, 522.
Nassau, J. J., Blanco, V. M., and Morgan, W. W. 1954, *Ap. J.*, **120**, 478.
Neugebauer, G., and Leighton, R. B. 1969, *Two Micron Sky Survey* (NASA SP-3047) (TMSS).
Noguchi, K., Kawara, K., Kobayashi, Y., Okuda, H., Sato, S., and Oishi, M. 1981, *Pub. Astr. Soc. Japan*, **33**, 373.
Olofsson, H., Eriksson, K., and Gustafsson, B. 1987, *Astr. Ap.*, submitted.
Payne-Gaposchkin, C., and Whitney, C. A. 1976, *Smithsonian Ap. Obs. Spec. Rept.*, No. 370.
Poulakos, G. 1978, *Astr. Ap. Suppl.*, **32**, 395.
Price, S. D., and Murdock, T. L. 1983, *The Revised AFGL Infrared Sky Survey Catalog* (AFGL-TR-83-0161).
Richer, H. B. 1981, *Ap. J.*, **243**, 744.
Schechter, P. L., Aaronson, M., Blanco, V. M., and Cook, K. 1987, in preparation.
Sopka, R. J., Hildebrand, R., Jaffe, D. T., Gatley, I., Roellig, T., Werner, M., Jura, M., and Zuckerman, B. 1985, *Ap. J.*, **294**, 242.
Stephenson, C. B. 1973, *Pub. Warner and Swasey Obs.*, Vol. **1**, No. 4.
Thronson, H. A., Latter, W. B., Black, J. H., Bally, J., and Hacking, P. 1987, *Ap. J.*, **322**, in press.
Vogt, S. S. 1973, *A.J.*, **78**, 389.
Westerlund, B. 1971, *Astr. Ap. Suppl.*, **4**, 51.
Willems, F. J., and de Jong, T. 1986, *Ap. J.* (*Letters*), **309**, L39.
Wing, R. F., and Yorka, S. B. 1977, *M.N.R.A.S*, **178**, 383.
Wood, P. R. 1985, in *Cool Stars with Excesses of Heavy Elements*, ed. M. Jaschek and P. C. Keenan (Dordrecht: Reidel), p. 357.
Wyckoff, S., and Wehinger, P. 1974, *Pub. A.S.P.*, **86**, 464.
Zuckerman, B., and Aller, L. H. 1986, *Ap. J.*, **301**, 772.
Zuckerman, B., and Dyck, H. M. 1986*a*, *Ap. J.*, **304**, 394.
_____. 1986*b*, *Ap. J.*, **311**, 345.
Zuckerman, B., Dyck, H. M., and Claussen, M. J. 1986, *Ap. J.*, **304**, 401.
Zuckerman, B., Palmer, P., Gilra, D. F., Turner, B. E., and Morris, M. 1978, *Ap. J.* (*Letters*), **220**, L53.

M. J. CLAUSSEN and S. G. KLEINMANN: Department of Physics and Astronomy, 619 Lederle Graduate Research Center, University of Massachusetts, Amherst, MA 01003

R. R. JOYCE: Kitt Peak National Observatory, P.O. Box 26732, Tucson, AZ 85726

M. JURA: Department of Astronomy, University of California, Los Angeles, CA 90024